

Review

Structured Perovskite-Based Catalysts and Their Application as Three-Way Catalytic Converters—A Review

Sylvain Keav¹, Santhosh Kumar Matam¹, Davide Ferri² and Anke Weidenkaff^{1,3,*}

¹ Empa, Swiss Federal Laboratories for Materials Science and Technology, Laboratory for Solid State Chemistry and Catalysis, Ueberlandstrasse 129, Dübendorf CH-8600, Switzerland; E-Mails: sylvain.keav@outlook.fr (S.K.); santhosh.matam@empa.ch (S.K.M.)

² Paul Scherrer Institut, Villigen CH-5232, Switzerland; E-Mail: davide.ferri@psi.ch

³ Materials Chemistry, Institute for Materials Science, University of Stuttgart, Heisenbergstrasse 3, Stuttgart DE-70569, Germany

* Author to whom correspondence should be addressed; E-Mail: weidenkaff@imw.uni-stuttgart.de; Tel.: +49-0-711-685-61932; Fax: +49-0-711-685-51985.

Received: 14 March 2014; in revised form: 9 June 2014 / Accepted: 11 June 2014 /

Published: 1 July 2014

Abstract: Automotive Three-Way Catalysts (TWC) were introduced more than 40 years ago. Despite that, the development of a sustainable TWC still remains a critical research topic owing to the increasingly stringent emission regulations together with the price and scarcity of precious metals. Among other material classes, perovskite-type oxides are known to be valuable alternatives to conventionally used TWC compositions and have demonstrated to be suitable for a wide range of automotive applications, ranging from TWC to Diesel Oxidation Catalysts (DOC), from NO_x Storage Reduction catalysts (NSR) to soot combustion catalysts. The interest in these catalysts has been revitalized in the past ten years by the introduction of the concept of catalyst regenerability of perovskite-based TWC, which is in principle well applicable to other catalytic processes as well, and by the possibility to reduce the amounts of critical elements, such as precious metals without seriously lowering the catalytic performance. The aim of this review is to show that perovskite-type oxides have the potential to fulfil the requirements (high activity, stability, and possibility to be included into structured catalysts) for implementation in TWC.

Keywords: perovskite-type oxides; honeycombs; structured catalysts; three-way catalysts; CO oxidation; hydrocarbon combustion; NO_x reduction; self-regenerative properties; washcoat

1. Introduction

Unburnt hydrocarbons (UHC), carbon monoxide (CO), and nitrogen oxides (NO_x) are the major noxious gases present in the exhaust of internal combustion engines. In order to comply with the stringent emission levels imposed by the legislation, these compounds have to be eliminated before they are released into the surrounding environment. For this purpose, gasoline-powered vehicles are equipped with a Three-Way Catalytic (TWC) converter. This emission control device, constituted of a mixture of catalytically active components deposited onto a monolithic honeycomb substrate, allows the simultaneous conversion of UHC, CO, and NO_x into harmless CO₂, H₂O, and N₂ (Equations (1)–(4)).



Because oxidation and reduction reactions must occur simultaneously, TWC are most efficient when operated under conditions close to the stoichiometric point (*i.e.*, air-to-fuel ratio of 14.7 w/w for gasoline vehicles). The composition of the exhaust is continuously determined by an oxygen sensor and the air-to-fuel ratio is adjusted accordingly by the fuel-control feedback system. A time lag between the analysis and the adjustment produces slight redox fluctuations of the exhaust gas composition around the stoichiometry [1].

The current TWC technology used in gasoline vehicles is based on noble metals. Platinum and palladium are used as oxidation components. Both can also contribute to NO_x reduction but are much less efficient than rhodium. The performance of the noble metals is increased by dispersion on a high specific surface area (*ca.* 100 m²·g⁻¹) γ-Al₂O₃ support. Ceria-zirconia, a high Oxygen Storage Capacity (OSC) material was introduced to minimize the air-to-fuel ratio fluctuations in the exhaust [2]. Other common additives include BaO (NO_x trap), zeolites (UHC or NO_x adsorbent), La₂O₃ (thermal stability enhancer for γ-Al₂O₃), TiO₂, NiO and SiO₂. Natural gas vehicles (NGV) generate exhaust emissions containing higher concentrations of methane, a potent greenhouse gas [3] and the most difficult hydrocarbon to oxidize, with respect to their gasoline counterparts. For this reason, TWC for NGV are mainly based on Pd, the most active catalyst for methane oxidation, and contain a threefold higher noble metal loading (*ca.* 3 mg·cm⁻³) than their gasoline equivalents (*ca.* 1 mg·cm⁻³) [4].

TWC are more exposed to high temperatures (up to 1000 °C) than diesel oxidation catalysts as a consequence of their vicinity to the engine or of the higher fuel load during operation. Consequently, thermal ageing can cause noble metal sintering processes or diffusion into the alumina support with mileage [5]. Because of the progressive loss of catalytic activity upon ageing and of the price and scarcity of noble metals, there is a need to further develop this technology for limiting their amount in the catalytic converter and for increasing their tolerance to the harsh operating conditions.

Already, in 1971, LaCoO₃ perovskite-type oxide was proposed as an economic substitute for noble metal-based exhaust after treatment catalysts [6]. Co-, Fe-, Mn-, and Ru-based perovskite-type oxides exhibited promising activity for the oxidation of CO and the reduction of NO_x [7–11]. La_{0.8}Sr_{0.2}CoO₃ was shown to compare well with 1 wt% Pt/Al₂O₃ for hydrocarbon oxidation [12]. The promising

oxygen storage capacity of $\text{LaMn}_{0.976}\text{Rh}_{0.024}\text{O}_{3+\delta}$ was also pointed out [13]. However, the high levels of sulfur in the fuels greatly limited their use in real applications. Recently, the use of $\text{LaFe}_{0.95}\text{Pd}_{0.05}\text{O}_3$ [14] for the exhaust after treatment of gasoline engines and the demonstration that $\text{La}_{0.9}\text{Sr}_{0.1}\text{CoO}_3$ can rival with noble metal-based catalysts for the treatment of diesel vehicle exhaust [15] confirmed the suitability of and rejuvenated the interest for this class of catalysts. Over the past several years, a continuous effort was undertaken to understand and improve the catalytic properties of perovskite-type oxides in automotive applications. In this review, we briefly describe the redox properties of perovskite-type oxides and the relevant mechanisms involved in oxidation and reduction reactions peculiar of TWC operation. Because of our interest in catalytic converters for NGV applications, the main part of the review is dedicated to the practical aspects of the use of structured perovskite-type oxide catalysts with a special emphasis on TWC. The advantages and limits will be discussed with the aim of identifying the most suitable types of catalysts for automotive applications.

2. Perovskite-Type Oxides

Perovskite-type oxides with the general formula ABO_3 can crystallise in cubic structure with a space group Pmm or in distorted orthorhombic, rhombohedral, tetragonal, monoclinic or triclinic symmetry. The content of oxygen and defects can vary depending on the composition due to a large stability range of the structure. The larger A-site cation is often a rare earth (La, Sm, Pr), an alkaline earth (Sr, Ba, Ca), or an alkali (Na, K) metal cation coordinated to 12 oxygen anions. The B-site cation is typically a smaller transition metal cation occupying octahedral interstices in the oxygen framework. The stability of the perovskite phases is largely governed by geometric considerations that are best summarized by the Goldschmidt tolerance factor, t (Equation (5)):

$$t = \frac{(r_A + r_O)}{\sqrt{2}(r_B + r_O)} \quad (5)$$

where r_A , r_B , and r_O are the respective radii of A, B, and oxygen ions. The value of the Goldschmidt tolerance factor must be in the range from 0.75 to 1.00 in order to obtain the perovskite structure [16]. Several combinations of A- and B-site cations can form a stable perovskite-like structure. Additionally, A- and B-site cations, as well as oxygen anions can be partially substituted by other suitable elements [17,18]. Partial substitution allows the control of the valence state of A- and B-site cations as well as the non-stoichiometry (cationic or anionic vacancies) in the mixed oxide based on electroneutrality arguments. The presence of a multiplicity of oxidation states is the major responsible for the catalytic properties of perovskite-type catalysts [19,20]. Due to this wide diversity, perovskite-type oxides also offer a large array of properties [21] (e.g., ferroelectricity, piezoelectricity, pyroelectricity, thermoelectricity [22], magnetism, superconductivity), which can be finely tuned for intended applications. For these reasons, more than 2000 scientific papers are devoted to perovskite-type materials every year and several review articles specifically focus on their preparation, structure elucidation, and applications [23–27].

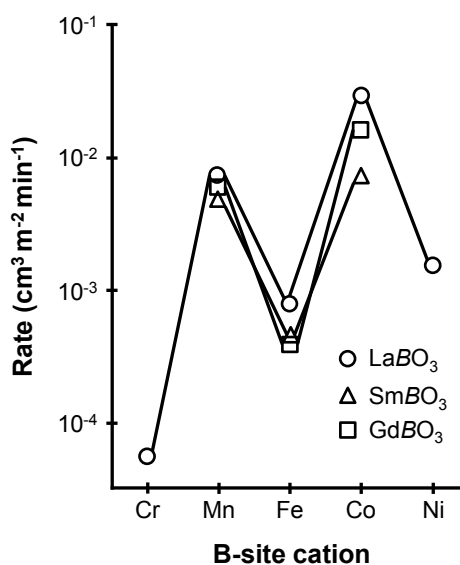
Perovskite-type oxides possess adsorption, acid-base, as well as redox properties, which lead to attractive catalytic properties [25]. The very first studies concerning their use as catalysts were conducted by Parravano *et al.* [28] and Dickens *et al.* [29] in 1952 and 1965, respectively. Since then, they were evaluated in various catalytic (e.g., total or partial oxidation of hydrocarbons, oxygenated

compounds or halocompounds; hydrogenation of CO or CO₂; hydrogenolysis of hydrocarbons), photocatalytic and electrocatalytic processes [25].

2.1. Parameters Influencing the Catalytic Activity

The catalytic activity of perovskite-type oxides is largely controlled by the nature of the B-site cation. Amongst noble metal-free perovskites, those based on Co and Mn perform the best in the oxidation of hydrocarbons and CO (Figure 1) [30–32]. The role of the A-site cation was found to be less decisive in the studied systems. Nitadori *et al.* [31], as well as Panich *et al.* [32], did not observe significant activity differences between Y-, La-, Pr-, Nd-, Sm-, Eu-, and Gd-based cobaltates tested in the oxidation of propane, methanol, CO, ethylbenzene, and propylene (Figure 1). However, partial substitution at the A-site by a cation of different valence (e.g., substitution of La³⁺ by Sr²⁺ or K⁺) can form oxygen vacancies and/or change the oxidation state of the B-site cation, which enhances substantially the catalytic properties of the material [31,33]. Detailed review concerning the effects of substitution on the CO oxidation activity of perovskite-type oxides can be found in reference [27].

Figure 1. Influence of A- and B-site cations on the catalytic activity of perovskite-type oxides for propane oxidation at 227 °C (Remark: B in LaBO₃, SmBO₃ and GdBO₃ refers to the B-site metal cation and not to boron element). Adapted with permission from Nitadori *et al.* [31]. Copyright 1988, The Chemical Society of Japan.



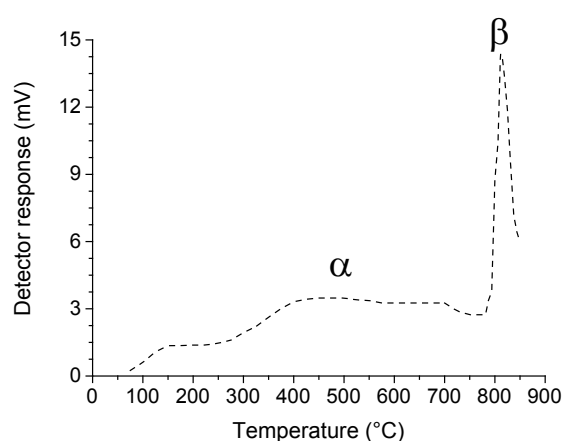
The performance does not only depend on the phase composition of the mixed oxide but also on the preparation procedure and its parameters, as these affect the crystallinity, texture and morphology of the final material [34–39]. For example, the TWC activity of La_{0.7}Sr_{0.3}Mn_{0.7}Cu_{0.3}O_{3-δ} prepared by complexation of nitrate salts in the presence of citric acid and ammonia is strongly affected by the acid-to-ammonia ratio employed for the synthesis [40] since it affects the polymerization of the precursor molecules. The catalytic performance of perovskite-type oxides is well-known to increase with their Specific Surface Area (SSA) [11,23] which can often be very low. The main reason for this is that perovskite-type oxides are essentially high temperature phases and most of their preparation procedures require heating up at relatively high temperature. Solution chemistry methods (sol-gel,

freeze-drying, spray-drying, co-precipitation, *etc.*) can generally produce highly crystalline materials at lower temperature (700–800 °C) than solid-state reaction (900–1000 °C). Consequently, materials prepared by such means are usually preferred for catalytic applications because they have a larger SSA (up to 30 m²·g⁻¹ compared to less than 2 m²·g⁻¹). As an exception to this rule, a solid state reaction method designated as reactive grinding, which was developed by the group of Kaliaguine in the late 1990s [41–45], proved to be efficient in producing perovskite-type oxides with high SSA. This low-temperature mechano-synthesis procedure consists in the high-energy ball-milling of oxide precursors for several hours at a temperature lower than 40 °C. The so-formed low SSA perovskite-type phase is subsequently ball-milled in the presence of a non-reactive additive (*i.e.*, ZnO) which is leached at the end of the synthesis [46] to obtain a high SSA (sometimes above 100 m²·g⁻¹ [42]) material.

2.2. Reaction Mechanisms

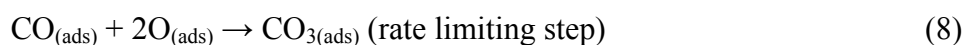
The high TWC performance of perovskite-type oxides is related to their oxygen mobility and storage capacity. Certain compounds, such as LaMn_{1-x}Ni_xO₃, even demonstrate significantly higher OSC than commercial ceria-zirconia [47]. Oxygen uptake and release is associated with the existence of structural defects and the change of the oxidation state of the B-site cation. Some perovskite-type materials are employed as supports for high redox potential oxides which are chemically incompatible with conventional γ -Al₂O₃. For example, MnO_x/LaAlO₃ is characterized by a promisingly high OSC [48]. Because two types of catalytically active oxygen species co-exist in a perovskite-type oxide (Figure 2) [49], two redox mechanisms have been proposed. Suprafacial oxygen species (α) are adsorbed on the oxide surface and are available at low temperature, generally below 600 °C. At higher temperature, bulk oxygen from the lattice, referred to as intrafacial oxygen (β), is activated and takes part in the catalytic reaction according to a Mars-van-Krevelen mechanism. In both cases, dissociation of molecular oxygen (or NO) from the gas phase must replenish oxygen species from the material, which are consumed during the reaction, so that the latter can proceed [13].

Figure 2. Oxygen temperature-programmed desorption on La_{0.6}Sr_{0.4}CoO₃. The broad low-temperature desorption peak corresponds to α -oxygen species and the sharp high-temperature one to β -oxygen species. Adapted with permission from Yamazoe *et al.* [49]. Copyright 1981, The Chemical Society of Japan.

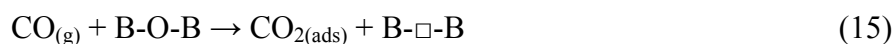
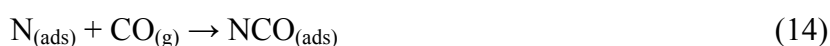


Oxidation of hydrocarbons by molecular oxygen is governed either by a suprafacial or an intrafacial mechanism. The combustion of propylene and iso-butene on LaBO_3 ($B = \text{Cr, Mn, Fe, Co, and Ni}$) at 250 °C occurs through a suprafacial process [50]. Methane oxidation takes place according to a suprafacial mechanism below 800 °C and according to an intrafacial one at higher temperature [51]. The combustion of toluene on LaFeO_3 and YFeO_3 is probably a suprafacial reaction, although the scenario of an intrafacial mechanism cannot be ruled out in the case of the latter oxide [52].

CO oxidation by molecular oxygen is recognized to occur through a suprafacial process [26,53,54]. The reaction (Equations (8)–(10)) takes place between oxygen species dissociatively adsorbed on surface B metal cations (Equation (6)) and CO species non-dissociatively adsorbed on O^{2-} anions (Equation (7)) [55,56]. In agreement with its limited influence on activity, the A-site cation does not seem to be involved in adsorption and reaction.



NO reduction takes place following an intrafacial mechanism [9,25,33,53,54]. NO dissociatively adsorbs on a surface oxygen vacancy (\square) (Equation (11)). The recombination of two adsorbed nitrogen species leads to the formation of N_2 (Equation (12)) while parallel pathways produce undesired N_2O (Equation (13)) and isocyanate species (Equation (14)) [57]. The oxygen vacancy is restored by the reducing species in the gas phase (e.g., CO (Equation (15))). It has to be noted that, on perovskite-type oxides containing redox-active B-site cations (e.g., Co, Ni), the consumption of O_2 proceeds preferentially to that of NO when both oxidizing species are present in the gas phase [58].



2.3. Incorporation of a Noble Metal

Despite the promising TWC performance of perovskite-type oxides, their very low SSA and their reactivity with typical components of three-way catalytic converters (e.g., $\gamma\text{-Al}_2\text{O}_3$) have to be overcome by the development of appropriate strategies. These issues will be developed in more details further in the article. The low price of noble metal-free perovskite-type oxides is counterbalanced by some of their limits, which appear critical for their implementation in real TWC. Most of these materials have a very low resistance against sulfur-containing poisons and those that do not (e.g., the LaCrO_3 class) generally provide insufficient overall performance (Figure 3) [10,59,60]. The partial

substitution of the B-site cation by a noble metal dramatically increases the sulfur tolerance of perovskite-type oxides [61]. Tzimpilis *et al.* reported the activation of a $\text{La}_{1.034}\text{Mn}_{0.966}\text{Pd}_{0.05}\text{O}_z$ catalyst in the presence of 8 ppm of SO_2 [62,63]. Regardless of their promising performance, noble metal-free perovskite type oxides still remain less active than noble metal supported catalysts [64]. Their operating window (range of exhaust compositions around the stoichiometry at which high conversions of UHC, CO, and NO_x are simultaneously reached) is also much narrower (Figure 4) [65]. The incorporation of small amounts of a noble metal in the perovskite significantly promotes the reduction of NO_x (which is otherwise limited) and improves the low temperature oxidation of UHC and CO (Figure 5) [13,66,67] (note the difference of reaction temperature and the inversion of the x axis between Figures 4 and 5). Some noble metal-based perovskite-type oxides present additional advantages (e.g., better selectivity [64], activity improvement in the presence of water [68]) compared to conventional TWC. Furthermore, the incorporation of the noble metal in the perovskite matrix protects it against sintering and reduces its losses by volatilization under oxidizing atmosphere [9,69].

Figure 3. TWC performance of LaCoO_3 and LaCrO_3 at 550 °C and 32,500 h^{-1} during ageing under an oxygen-rich sulfur-containing atmosphere. Adapted with permission from Jovanovic *et al.* [60]. Copyright 1991, Elsevier.

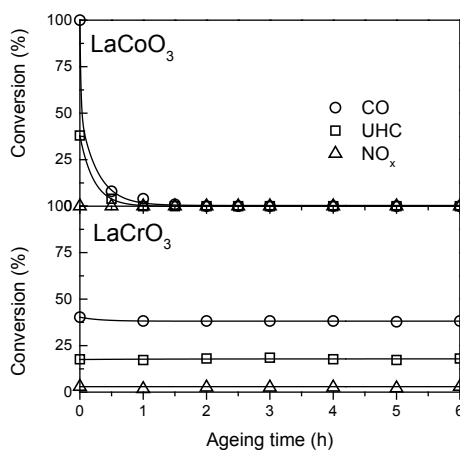


Figure 4. TWC activity of LaCoO_3 at 655–685 °C and 18,000–21,500 h^{-1} as a function of CO concentration in the exhaust gases (the percent of CO in the exhaust is indicative of the air-to fuel ratio). Adapted with permission from Sorenson *et al.* [65]. Copyright 1974, The American Ceramic Society.

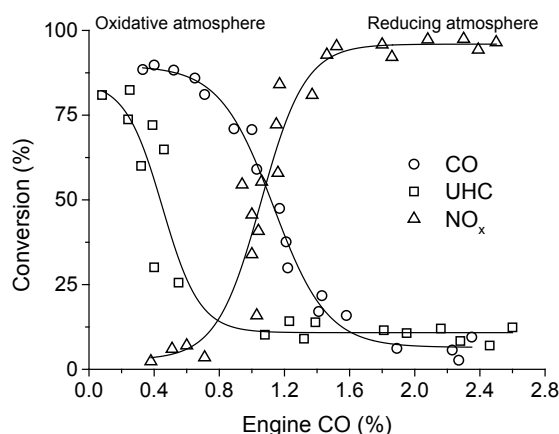
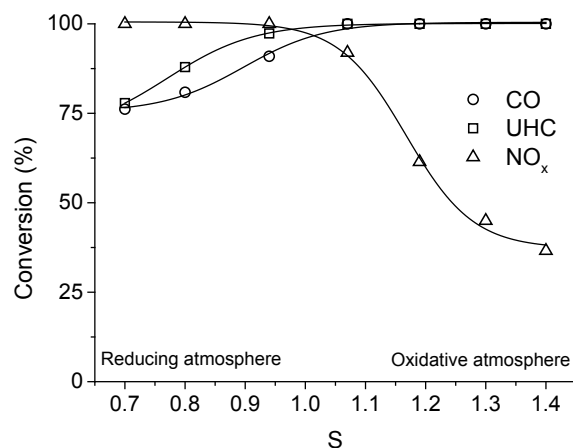


Figure 5. TWC activity of $\text{LaMn}_{0.976}\text{Rh}_{0.024}\text{O}_{3+\delta}$ at 400 °C and 13,000 h^{-1} as a function of the stoichiometric factor $\left(S = \frac{2 \cdot C_{\text{O}_2} + C_{\text{NO}}}{C_{\text{CO}} + 9 \cdot C_{\text{C}_3\text{H}_6}}\right)$. Adapted with permission from Guilhaume *et al.* [13]. Copyright 1997, Elsevier.



The interest in perovskite-type oxides for TWC applications was intensified in the early 2000s with the discovery of the so-called self-regenerative property [70,71]. The high temperature (up to 1000 °C) and the redox environment of exhaust gases are known to provoke the progressive deactivation of conventional supported noble metal catalysts. This loss of activity, which results from the agglomeration and growth of metal particles, is claimed to be suppressed in self-regenerative perovskite-based catalysts. The self-regenerative function was first reported on $\text{LaFe}_{0.57}\text{Co}_{0.38}\text{Pd}_{0.05}\text{O}_3$ [70] in which palladium (but also a small fraction of cobalt) oscillates between two oxidation and coordination states depending on the redox environment. Under slightly oxidative atmosphere, it is incorporated in the perovskite lattice as Pd^{3+} cations occupying B-sites. Under slightly reducing environment, it segregates out of the perovskite crystal in the form of metallic nanoparticles of 1–3 nm. Therefore, palladium reversibly moves in and out of the perovskite matrix in response to the cyclic redox fluctuations of the exhaust gas composition. These reversible structural changes, which are fast (only a few seconds at 600 °C [14]) and occur even at low temperature (100–400 °C) [72,73], suppress the growth of Pd particles compared to $\text{Pd}/\text{Al}_2\text{O}_3$. To illustrate this phenomenon, the behaviors of two catalysts of similar initial activity are compared after ageing in a real exhaust at 900 °C for 100 h. The reference $\text{Pd}/\gamma\text{-Al}_2\text{O}_3$ catalyst loses about 10% of its activity (Figure 6) owing to the sintering of noble metal particles ($D > 100$ nm). On the contrary, $\text{LaFe}_{0.57}\text{Co}_{0.38}\text{Pd}_{0.05}\text{O}_3$ maintains a high Pd dispersion ($D = 1\text{--}3$ nm) and its activity remains unchanged (Figure 6) [70,74]. Following the discovery of the self-regenerative property of $\text{LaFe}_{0.57}\text{Co}_{0.38}\text{Pd}_{0.05}\text{O}_3$, several other “intelligent” catalysts based on platinum or rhodium hosted in LaFeO_3 , LaAlO_3 , CaTiO_3 , CaZrO_3 , SrTiO_3 , SrZrO_3 , BaTiO_3 , or BaZrO_3 structure were identified [75]. Each combination of noble metal and host structure is characterized by the proportion of precious metal likely to form a solid solution with the perovskite-type oxide and, therefore, to be involved in the self-regeneration process (Table 1) [75]. The stronger metal-support interaction of the noble metal with a perovskite-type oxide support, as compared to a conventional alumina support, significantly increases its resistance to thermal sintering, allowing to enhance the catalytic performance while minimizing the noble metal content [76,77].

Figure 6. Change in the CO-NO_x cross-over point conversion (which is indicative of the catalytic activity) of LaFe_{0.57}Co_{0.38}Pd_{0.05}O₃ and Pd/Al₂O₃ catalysts upon ageing in a real exhaust gas at 900 °C for 100 h. Adapted with permission from Nishihata *et al.* [70]. Copyright 2002, Nature Publishing Group.

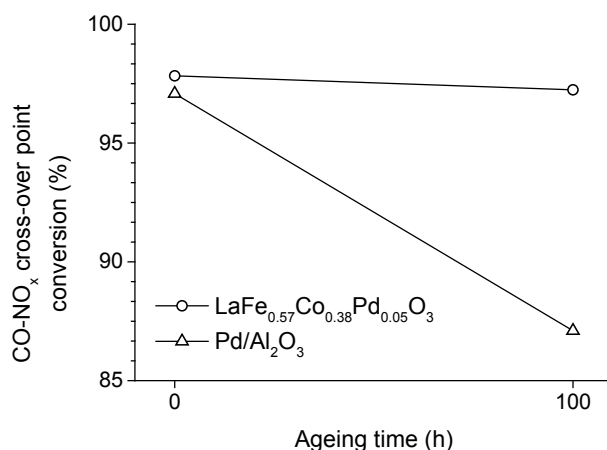


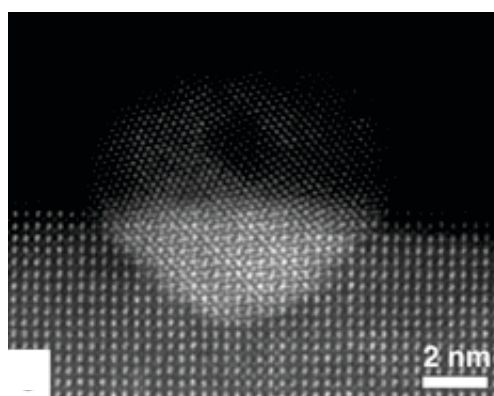
Table 1. Proportion of noble metal in AB_{0.95}B'_{0.05}O₃ (B' = Pd, Pt, Rh) actually forming a solid solution with the host structure under reducing (lower value) or oxidative (upper value) atmosphere (“-” indicates that no data is available; “x” indicates that the precious metal and the perovskite do not form a solid solution). Adapted from Tanaka *et al.* [75].

Host structure	Noble metal		
	Pd	Rh	Pt
LaFeO ₃	0%–100%	63%–100%	25%–83%
LaAlO ₃	-	69%–100%	-
CaTiO ₃	x	28%–100%	20%–100%
CaZrO ₃	-	53%–100%	27%–100%
SrTiO ₃	-	37%–100%	50%–100%
SrZrO ₃	-	x	x
BaTiO ₃	-	0%–100%	25%–93% ^o
BaZrO ₃	-	47%–100%	x

Recent HAADF-STEM observations on Pd-LaFeO₃, Pt-CaTiO₃, Rh-CaTiO₃, and Pt-BaCeO₃ systems question the self-regenerative function [78,79]. The microscopy study evidenced that a fraction of the fully reversible formation-dissolution of noble metal particles under redox cycling predominantly takes place within the bulk of the host structure. This implies that most of the metallic clusters formed under reducing atmosphere are not directly accessible to the catalytic reaction. However, it should be kept in mind that the easy A⁰ ↔ A³⁺ (A = Pd, Pt, Rh) transformation is accompanied by an oxygen uptake-release and that a defective perovskite structure is formed when the noble metal segregates out of the oxide. Both phenomena undoubtedly play a role in the activity of the material. The formation and dissolution of noble metal clusters at the surface of the perovskite particles was found to be much more limited than expected [78]. The surface noble metal clusters formed after reduction in 10 vol% H₂/N₂ at 800 °C for 1 h tended to coarsen rather than return into the perovskite matrix after oxidation in 20 vol% O₂/N₂ at 800 °C for 1 h [79]. At least, the partial

embedding of these particles in the support surface confirms that they strongly interact with the host structure (Figure 7) [78]. In fact, contrary to what happens during the relatively long pretreatment procedure prior to HAADF-STEM observation (1 h under constant atmosphere [79] or alternance between reducing and oxidizing environments every 10 min [78]), one can expect that this interaction should be constantly revived under the high frequency (0.5–5 Hz) redox fluctuations of a real exhaust. This should limit the mobility of the precious metal particles on the surface of the host material and prevent their agglomeration. Therefore, it is likely that the durability of “self-regenerative” materials does not originate from a fully reversible phenomenon but from a strong interaction between surface precious metal particles and the perovskite surface maintaining them in a highly dispersed state under real operating conditions.

Figure 7. TEM image of a Pd particle partially embedded in the surface of a LaFeO₃ support. Reproduced with permission from Katz *et al.* [78]. Copyright 2011, American Chemical Society.



A last point worth mentioning is that the incorporation of the noble metal in the perovskite matrix is not beneficial for all applications. Indeed, perovskite-supported noble metal catalysts remain more active than noble metal-substituted perovskites [80]. As a consequence, Pd-based perovskite-type oxides tested in the treatment of NGV exhaust were found to deactivate upon thermal treatment at high temperature (850–950 °C) due to the migration of Pd out of the perovskite lattice [63] and the growth of noble metal particles [81].

3. Preparation of Structured Catalysts

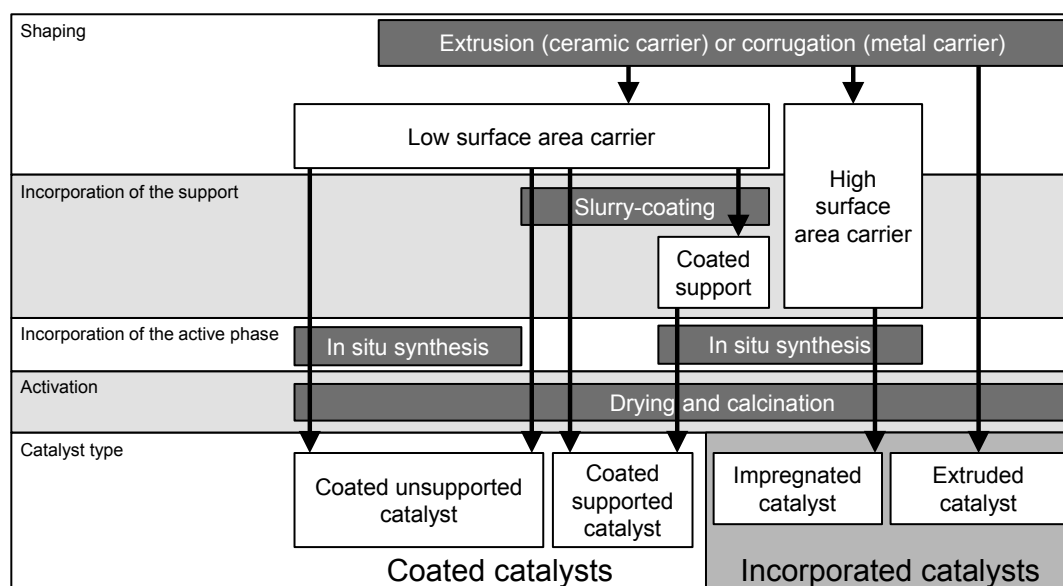
TWC for automotive applications are traditionally supported on a structured carrier. Structured catalysts offer several advantages compared to their powder and pellet counterparts. These include (i) a very low pressure drop; (ii) an increased efficiency due to an improved mass transfer; (iii) a high safety (self-draining reactor, no risk of clogging); (iv) an easy separation from the reaction medium and (v) cost reduction (low production costs, low catalyst loadings) [82,83]. The requirements, preparation procedures and performance of structured catalysts have been discussed in several review articles [82–85]. The most common structured carriers are monoliths, also referred to as honeycombs. These single block structures possess numerous small parallel straight channels which can be of square, triangular, hexagonal or round shape. Channel density can vary from 25 to 1600 channels per square inch (cpsi) and has to be carefully chosen depending on the specific requirements of the process. A higher cell

density implies a higher geometric surface area but also more complex manufacturing and washcoating procedures as well as higher pressure drops [82]. Monolith substrates used in automotive applications generally have square channels with a cell density of 300–600 cpsi [86,87]. More than 90% are made of cordierite ($2\text{MgO}\cdot 2\text{Al}_2\text{O}_3\cdot 5\text{SiO}_2$) [83], which offers high mechanical strength, very low thermal expansion coefficient and resistance to high temperatures and thermal shocks [82,85,86]. Other ceramic materials (mullite, silicon carbide, alumina, *etc.*) or metals (Al, Ni, stainless steel, FeCrAl alloy, *etc.*) are also used in practice [82,83,85].

In the previous sections of this review, we have demonstrated that perovskite-type materials show promising activities in the combustion of hydrocarbons, oxidation of CO and reduction of NO_x . In order to confirm their potential for real application in TWC converters, it is necessary to evaluate their performance as active components of structured catalysts. Amongst the extensive literature related to perovskite-type catalysts, studies concerning specifically structured ones are still relatively scarce. Furthermore, the great majority is dedicated to the oxidation of CO or various hydrocarbons under lean atmosphere and at relatively low gas hourly space velocity ($\text{GHSV} < 10,000 \text{ h}^{-1}$). It is therefore difficult, from these data, to assess the performance of perovskite-type catalysts in TWC converters, whose operating conditions (stoichiometric atmosphere, GHSV up to $100,000 \text{ h}^{-1}$) significantly deviate from those previously mentioned.

In the following, we will refer to the two main categories of structured catalysts described by Avila *et al.* [85] (Figure 8), namely incorporated and coated catalysts.

Figure 8. Paths for the preparation of structured perovskite catalysts. Adapted with permission from a more general scheme by Avila *et al.* [85]. Copyright 2005, Elsevier.



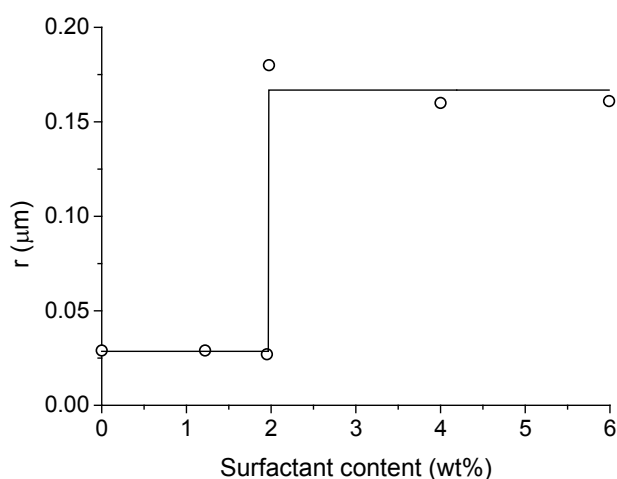
3.1. Incorporated Catalysts

In incorporated catalysts, the active phase is an integral part of the structured body. Consequently, a high mass of the active component is present and a first requirement is therefore that the catalytic material should not be too expensive. Because of their nature, they become relevant to conditions where catalyst erosion can occur and diffusion limitations are negligible. They are produced either by

direct extrusion of a plastic paste containing the catalytic material or by impregnation of precursors on a high surface area substrate. To our knowledge, only perovskite-containing structured catalysts of the first category have been studied thus far. Most of available articles have been produced by the same group: Isupova, Sadykov *et al.* [88–93] prepared extruded monoliths from a wide range of perovskite catalyst compositions ($A = \text{La, Sr, Ce, Dy, Y}$; $B = \text{Fe, Mn, Ni, Co, Cu}$).

Perovskite-based monoliths can be produced in a reduced number of steps including the extrusion of a plastic paste containing the catalytic powder, a drying step and a calcination step. Even in the absence of additives, catalyst powders with sufficient surface reactivity (*i.e.*, high surface density of acid and hydroxyl groups) easily form a water-based paste from which high-strength extrudates can be produced [88]. In other cases, it is necessary to use additives in order to, on the one hand, adjust the rheological properties of the paste to make it suitable for the extrusion process and, on the other hand, optimize the mechanical strength and porosity of the final monolith. The use of an alumina binder enhances the contacts between perovskite particles, resulting in increased SSA, mechanical strength and resistance to thermal shocks [88–90]. In some cases, there can be counterproductive effects of employing a binder. A decrease of the catalytic activity can result from the partial blockage of active centers by alumina particles [89] or from the formation of less active hexa-aluminate surface micro-phases due to chemical interactions between the binder and the perovskite-type catalyst at high temperature [90]. In order to force the conversion of the alumina binder into a hexa-aluminate phase before it can alter the perovskite, sacrificial A- and/or B-site cations can be added to the extrusion paste as nitrate salts [91]. While small amounts of a surfactant (ethylene glycol, glycerol, carboxymethyl hydro cellulose) improve the rheological properties of the extrusion paste and limit the formation of cracks during drying, too high amounts are responsible for a significant increase of the mean pore size (Figure 9) and consequently a decrease of the mechanical strength [88,89]. The addition of ceramic fibers improves the resistance to thermal shocks [88] and modifies the pore structure of the monolith [91,92]. Organic or mineral acids can be used as peptizing agents. Despite that acetic acid is more environment-friendly than nitric acid (HNO_3 releases NO_x during the calcination step), monoliths with higher mechanical strength were produced with the latter [88,89].

Figure 9. Influence of surfactant (ethylene glycol) content on the mean pore radius of monolithic LaMnO_3 . Adapted with permission from Isupova *et al.* [88]. Copyright 1996, Elsevier.



The drying step has to be performed slowly under controlled humidity conditions in order to avoid the formation of cracks [89,90]. Extruded monoliths can contain up to 70–80 wt% of active phase. Appropriate formulation of the extrusion paste can yield high SSA ($30\text{--}75\text{ m}^2\cdot\text{g}^{-1}$), porosity (up to $0.3\text{ cm}^3\cdot\text{g}^{-1}$), and mechanical strength (up to $10\text{--}20\text{ MPa}\cdot\text{cm}^{-2}$), even after calcination at $900\text{ }^\circ\text{C}$. The extrusion procedure was not reported to alter the phase composition [91,92].

The catalytic performance of extruded perovskite catalysts was found to be mostly determined by their SSA [91,92]. Isupova *et al.* calculated that the specific rates of methane disappearance per gram of active component were comparable to those reported by other authors on powder and coated perovskite-type catalysts [92]. Therefore, an extruded catalyst, which, by its nature, contains a higher amount of active phase than a coated catalyst of comparable geometry (volume, density of channels, *etc.*) will show a higher overall activity in the kinetic regime [94]. Nevertheless, as active sites are distributed within the walls of the structured body, some of them are not easily accessible to the reactants and mass transfer limitations commonly occur at high temperature (e.g., above $560\text{ }^\circ\text{C}$ for methane oxidation [91,93]). High temperature (up to $1300\text{ }^\circ\text{C}$) tests on pilot installations during several months showed the better stability in terms of activity, mechanical strength, monolith integrity and resistance to poisons (HF, HCl, SO_2) of extruded perovskite-type catalysts compared to the coated oxide catalysts conventionally used for the same applications [88–90].

3.2. Coated Catalysts

Coated catalysts are obtained when a thin layer (*ca.* $100\text{ }\mu\text{m}$) of active components is deposited on the walls of a low surface area structured carrier. Although perovskite-type coatings can be obtained through plasma spraying [95], chemical vapor deposition [96], flame-assisted vapor deposition [97], physical vapor deposition [98] or even atomic layer deposition [99], these advanced techniques are not easily scalable, based on cost considerations, and generally produce dense layers which are not suitable for catalytic applications. We will, therefore, limit our discussion to more conventional and cost effective methods. Precursor techniques where the active material is synthesized directly on the substrate wall will be distinguished from procedures where a slurry of the powder catalyst is washcoated.

3.2.1. Precursor-Derived “On-Substrate-Wall” Synthesis of Catalysts

Immersion of the structured carrier in an aqueous solution of salt precursors in the absence of any additive [100,101] or in the presence of citric acid [102] is employed to prepare perovskite-type active phases directly on the substrate. Citric acid acts as a chelating agent and enables the preparation of highly concentrated precursor solutions. The increased viscosity and concentration of such solutions result in increased amounts of deposited material. A variation of this preparation protocol uses a polymerized solution of nitrate precursors, citric acid and ethylene glycol prepared by the Pechini method [101,103–105]. After withdrawal of the impregnated carrier, the excess solution is removed by blowing pressurized air. Drying can be carried out in a conventional furnace ($80\text{--}200\text{ }^\circ\text{C}$) [102–104], under air-flow at room temperature [101], or in a microwave oven [106]. The latter option allows a homogeneous drying, preventing the redistribution of the active material and therefore ensuring its good distribution on the carrier [107]. Finally, calcination at $700\text{--}1100\text{ }^\circ\text{C}$ [101,102,104] converts the precursors into the desired perovskite-type oxide. Phase pure materials are generally obtained but

secondary phases are sometimes detected [101]. However, the method presents some drawbacks. First, it is long, because several dip-dry-calcine cycles are required to obtain the desired active phase loading. Then, low SSA (below $6 \text{ m}^2\cdot\text{g}^{-1}$) of the synthesized perovskite-type materials is generally obtained [101,103,104]. In addition, the partial dissolution of the substrate in the acidic and chelating solution used for impregnation leads to the formation of less active secondary phases (e.g., spinels, partially substituted perovskites) [101,103,104]. This phenomenon can be limited by precoating a thin layer of ZrO_2 or Ln_2O_3 primer (Ln = mixture of La, Ce, Pr, Nd, Sm) on the structured carrier prior to the deposition of the perovskite phase [103].

Polymerized solutions prepared by the Pechini method produce a distinct active phase layer covering the walls of the structured carrier [101]. The coating has a thickness of 2–160 μm [101–103] and shows a coherent interface with the substrate which was interpreted as a sign of good adherence [101,102]. However, large cracks (up to 30 μm ; Figure 10a) were observed in the coating and no adherence assessment test was performed. Traditional wet impregnation with a solution of metal nitrate precursors does not produce a separate catalytic layer but the active component is uniformly distributed across the walls of the structured carrier [100,101]. Despite these differences in morphology, similar activities are measured on both types of samples [101]. However, in the presence of mass transfer limitations, samples prepared following the Pechini method exhibit higher performance due to the better accessibility to their active sites (active phase distributed at the surface of the monolith walls rather than within them).

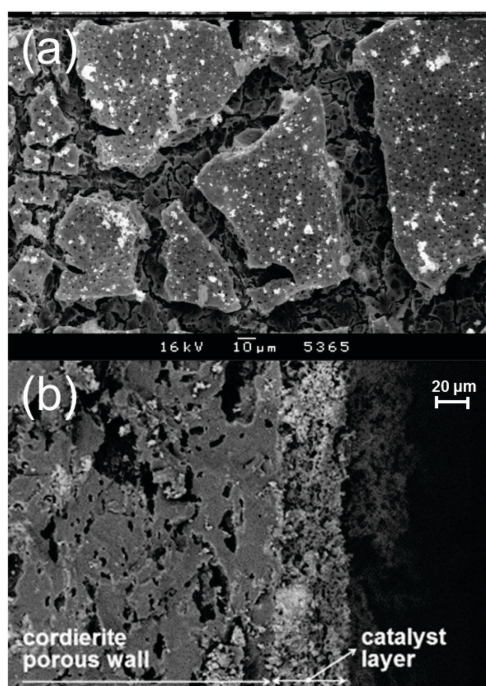
In situ solution combustion synthesis [4,108–116] seems to be a good alternative to the previously described procedures. It allows the production of a well-adhered and porous perovskite layer in a reduced number of steps. After being dipped into an aqueous solution containing nitrate precursors (oxidant), urea (fuel) and ammonium nitrate (combustion booster), the structured carrier is placed in an oven at 600–650 °C. This rapidly brings the aqueous phase to boil and the precursor mixture to ignite: within few minutes, the heat released by urea combustion allows the transformation of the nitrate precursors into a phase pure perovskite-type oxide [4,108–111]. The generation of large amounts of gaseous products in a very short period of time during the combustion produces a 40–100 μm thick, highly porous and spongy coating (Figure 10b) with high SSA ($4\text{--}30 \text{ m}^2\cdot\text{g}^{-1}$) [4,108–110,112,113]. Such a structure minimizes the pressure drops and improves the mass transfer [113]. Although catalytic powders prepared by solution combustion synthesis were reported to easily crumble [109,114], coatings obtained by the same procedure show excellent adherence. The weight loss of samples submitted to a vibration test consisting in a 5 h treatment in an ultrasonic bath is lower than 1% [4,110,112,113,115]. Thermal ageing at temperatures as high as 850 °C in the presence of SO_2 [115] or water [109] did not induce significant deactivation and no chemical interactions between the active phase and the structured carrier were evidenced [108–110,112,114–116].

3.2.2. Washcoated Catalysts

Washcoated catalysts are prepared from an already formed active phase powder which is used to produce a slurry and applied to the structured carrier surface by dip-coating. This technique consists in dipping the dry substrate into the catalyst suspension for a short period of time. After subsequent withdrawal, the excess slurry remaining in the channels/pores of the substrate is removed by blowing

pressurized air. The deposited catalyst layer is then left to dry between room temperature and 200 °C and finally fixed to the carrier by calcination at 500–700 °C.

Figure 10. SEM images of (a) a LaMnO_3 film prepared by CM (top-view) and (b) a $\text{La}_{0.8}\text{Li}_{0.2}\text{Cr}_{0.8}\text{O}_3$ layer deposited via solution combustion synthesis (cross-section). Reproduced with permission from Isupova *et al.* [101] and Fino *et al.* [112]. Copyright 2002 and 2006, Elsevier.

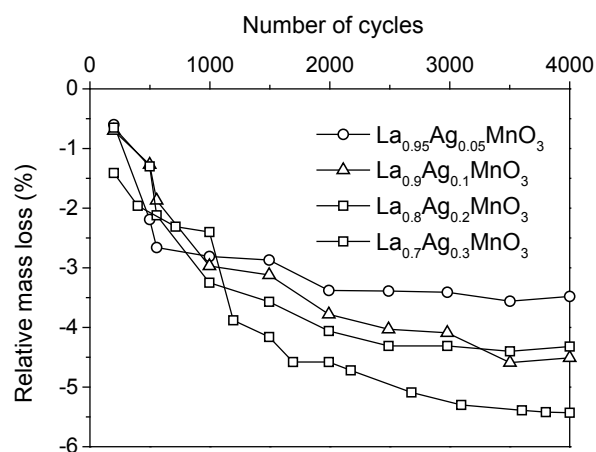


Washcoated Unsupported Catalysts

Perovskite-type materials used to prepare washcoated catalysts are generally obtained by conventional techniques such as the amorphous citrate method (CM) [106,117,118], co-precipitation [94,100,119] or flame-assisted synthesis (e.g., flame hydrolysis [118,120–122]). The solvent of the slurry is typically water [39,117,120–124] but organic solvents, such as *n*-butanol, are sometimes employed [62,63]. Similarly to extrusion pastes, various additives can be used to tune the rheological properties of the slurry and improve the quality of the coating. An alumina or zirconia binder increases the mechanical strength and adherence of the coated layer [106]. A temporary binder, such as Tylose (a cellulose derivative), can sometimes be employed [39,94,100,119]. This additive, which acts in the same way as a permanent binder, prevents damage that may occur during handling of the catalyst and is eliminated during the calcination step. A peptizer, such as nitric [117,120] or citric acid [125,126] improves the dispersion of suspended particles in the slurry. A critical parameter known to influence the stability of a slurry is the size of the suspended particles. If these particles are sufficiently small (*i.e.*, if the selected synthesis protocol produces very fine catalyst particles [121] or if an appropriate size fraction has formerly been collected through grinding and sieving [126]), they can be easily dispersed by low energy ball-milling [118,120–122] or even simple stirring at room temperature [117]. Otherwise, the slurry must be submitted to high energy ball-milling in order to attain catalyst particles of the desired size, typically below 5 μm [106].

Active phase layers deposited by dip-coating are generally homogeneously distributed over the surface of the carrier but cracks sometimes appear during drying, calcination [117] and operation. In the worst cases, the formation of deep cracks upon thermal ageing leads to the partial exfoliation of the active phase [122]. Therefore, besides catalytic activity, both the quality and adherence of the washcoat are important issues to be considered. The mechanical properties of the coated layer primarily depend on the characteristics of the initial catalyst powder. Perovskite-type materials with high SSA and good crystallinity can be obtained by CM after calcination at relatively low temperature (700–750 °C). Contrary to flame-made powders, such materials never experienced high temperatures and are characterized by a poor thermal stability. As a consequence, a coated CM-made perovskite powder is significantly deactivated after exposure to a temperature of 800 °C [120] and large cracks appear between the active phase and the carrier [118]. The composition of the mixed oxide is also of great importance because it influences the surface chemistry (e.g., nature and density of surface groups) of the oxide as well as the way the latter bonds to the carrier. For example, Kucharczyk *et al.* observed that the adherence of washcoated $\text{La}_{1-x}\text{Ag}_x\text{MnO}_3$ decreases with increasing the amount of Ag incorporated into the perovskite (Figure 11 [126]). Adherence obviously depends also on the nature of the substrate: the bonding of the catalyst is weaker on metal carriers, which have a much lower porosity and a smoother surface than ceramic ones [82,83,85,117].

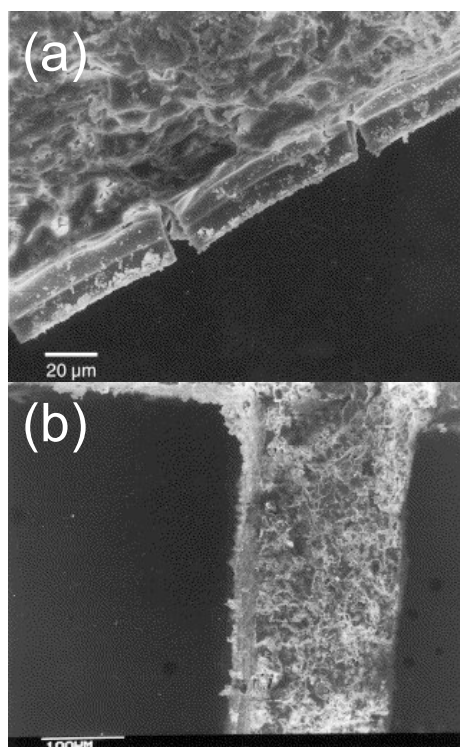
Figure 11. Influence of La substitution by Ag on the resistance of washcoated $\text{La}_{1-x}\text{Ag}_x\text{MnO}_3$ catalysts to 4000 cycles of heating to 1000 °C and rapid cooling to room temperature. Adapted with permission from Kucharczyk *et al.* [126]. Copyright 2008, Elsevier.



As previously mentioned, it is possible to improve the mechanical properties of the coated layer by means of additives. Qi *et al.* [106] observed that the mechanical strength of a coating consisting only of perovskite-based particles was so poor that it could simply be blown away by a strong nitrogen flow. Adherence was greatly improved through the addition of a binder. The grafting properties of the substrate, whether the latter is made of metal [125,126] or ceramic [120–122,126], can be greatly enhanced through the use of a primer. This very thin layer constituted of one or several oxide(s) (e.g., Al_2O_3 , TiO_2 , La_2O_3) is applied to the carrier prior to washcoat. It is generally obtained by dipping the substrate in a water-based sol [118,120,125,126] or an aqueous solution containing precursors [118]. The nanoparticles in the sol or the ions in the solution easily interact with the surface of the structured carrier, producing a well-adhered, dense oxide layer upon calcination. The increased

roughness of this primer, as compared to the original substrate, improves the bonding with the active phase [120]. Fabbrini *et al.* concluded that despite its much lower SSA, La_2O_3 constitutes a better primer than Al_2O_3 [121]. In fact, besides being prone to chemical interactions with the perovskite catalyst, the latter oxide has a poor thermal stability and its thermal expansion coefficient significantly differs from that of cordierite, favouring crack formation (Figure 12a,b) [118]. Lanthanum nitrate was found to be a better precursor of La_2O_3 than lanthanum acetate, the difference resting on their distinct decomposition behavior [121]. Lanthanum acetate tends to form platelet-shaped deposits, a morphology which is much less favorable to a good grafting of coated particles than the needle-like structures obtained when lanthanum nitrate is employed. Upon exposure to high temperature, lanthanum acetate agglomerates into larger plates, which can easily detach from the substrate, while lanthanum nitrate produces a compact layer ensuring the good anchoring of the active phase [121]. Catalytic layers deposited by slurry-coating were reported to be less adherent than those obtained by direct impregnation [106]. Therefore, a well-adhered perovskite coating obtained by *in situ* on-substrate-wall synthesis can also be used as an efficient primer [100]. Since this primer can have exactly the same formulation as the slurry-coated particles, a better adherence can be achieved while no deactivation due to chemical interactions can occur. From the available literature, it is unfortunately difficult to clearly identify the optimum parameters (slurry composition, active phase content, nature and amount of binder/primer, *etc.*) necessary to produce a well-adhered washcoat of a perovskite-type oxide. Beside the scarce quantification of the adherence properties in the available literature (Figure 11 [126]), the lack of a reference adherence assessment test makes it arduous to compare results obtained by different research groups.

Figure 12. SEM images of washcoated $\text{La}_{0.9}\text{Ce}_{0.1}\text{CoO}_3$ after accelerated ageing at 800 °C for 1 h: (a) Al_2O_3 primer and (b) La_2O_3 primer. Reproduced with permission from Fabbrini *et al.* [118]. Copyright 2003, Elsevier.



In addition to mechanical aspects, the chemical stability of the catalyst layer is also of great importance. In most cases, no changes of texture, crystallinity or composition occur during the dip-coating procedure [117]. Although surface modifications of the active phase (decrease of crystallinity, formation of surface hydroxyl groups) may take place during the preparation of the slurry, they are usually not critical for activity and thermal resistance [122]. As previously observed on extruded and *in situ* synthesized structured catalysts, chemical interactions between the active component and the substrate/binder/primer lead to the partial destruction of the perovskite structure and subsequent deactivation. For example, solid state reaction between the perovskite washcoat and the cordierite substrate [123], between La_2NiO_4 and the La_2O_3 primer [122], between $\text{La}_{0.8}\text{Ce}_{0.2}\text{NiO}_3$ and the ZrO_2 binder [106] or between LaCoO_3 and the Al_2O_3 primer [118] were reported.

In the absence of chemical incompatibilities, the main origin for the deactivation of washcoated unsupported perovskite-type catalysts is the reduction of their SSA [123,126]. Kucharczyk *et al.* reported that after 24 h of ageing at 900 °C, the methane conversion at 750 °C on monolith-carried $\text{La}_{0.8}\text{Ag}_{0.2}\text{MnO}_3$ decreased from 98.9% to 67.0% as SSA dropped from 29.4 to 1.7 $\text{m}^2\cdot\text{g}^{-1}$ [126]. Sufficient stability can be obtained through the use of appropriate synthesis procedure and binder/primer additives [120,126]: more than 90% of the initial activity of a $\text{La}_{0.9}\text{Ce}_{0.1}\text{CoO}_3$ washcoated catalyst could be maintained after ageing at 800 °C for 1 h [118,121]. Arendt *et al.* [117] reported that, at low temperature, perovskite-type catalysts were more active when carried on a metallic than on a ceramic substrate. The opposite behavior was observed at high temperature. Authors concluded that this could originate from the different thermal conductivity of the two carrier materials. However, since the catalyst particles adhered to the metal substrate (0.02–0.06 μm aggregates) were much smaller than those deposited on the ceramic one (3 μm aggregates), particle size effects cannot be excluded. The same authors observed that washcoated catalysts had increased activity compared to the corresponding powders. They suggested that the carrier material was able to activate molecular oxygen into strongly oxidizing species capable of limiting the accumulation of deactivating coke. On the contrary, Fabbrini, Forni *et al.* [118,120] calculated that, in the absence of a primer, the specific activity (per gram of active component) of carried catalysts, was lower than that of the corresponding powders, whereas identical activities were obtained when a primer was used.

Washcoated Supported Catalysts

Washcoated supported perovskite-type catalysts can be prepared by impregnation or deposition-precipitation of the active phase on an oxide support powder (e.g., $\gamma\text{-Al}_2\text{O}_3$, ZrO_2 , MgO) either before [39] or after [127–132] that the latter is washcoated on the structured carrier. This produces a homogeneously distributed active phase [127] on a porous support firmly anchored to the walls of the substrate [66,128].

Similarly to other types of coated catalysts, exposure to high temperature can cause fractures in the washcoat. Nevertheless, the latter were not reported to strongly reduce adherence [127,128]. ZrO_2 [128] and MgO [129] supports are chemically inert with respect to most of active phases. On the contrary, extensive interaction exists on $\gamma\text{-Al}_2\text{O}_3$ supported systems, which results, as earlier mentioned, in the formation of less active spinel structures, simple oxides and aluminate phases [66,130]. $\text{LaAl}_{11}\text{O}_{18}$ and $\text{LaCr}_{1-x}\text{Al}_x\text{O}_3$ form upon solid-state reaction between LaCrO_3 and $\gamma\text{-Al}_2\text{O}_3$ at high temperature [131]

while Mn from LaMnO₃ is incorporated in the alumina lattice even at low temperature [129]. Such chemical interactions can be limited by precoating a La₂O₃ layer on alumina prior to the application of the perovskite phase [66].

Deposition on a porous oxide support significantly increases the dispersion of the perovskite material, which enhances the catalytic performance [128,129,131]. Cimino *et al.* compared fresh unsupported and ZrO₂-supported LaMnO₃ monolithic catalysts. A three times higher specific rate of methane combustion per gram of catalyst (corresponding to a 14-fold increase in the specific rate per gram of active phase) was obtained on the supported system [128]. Activity enhancement is however not always so spectacular [119] and has a limit: large perovskite crystals form upon increase of the perovskite-type oxide loading and exposure to high temperatures, which leads to pore blocking and loss of dispersion [39,128–131]. The decrease of activity was reported to be proportional to the loss of specific surface area: a reduction of both these parameters by a factor four was observed after treating a monolithic γ -Al₂O₃ supported LaMnO₃ catalyst for 9 h at 1100 °C [127]. Although no support-active phase interactions were evidenced in the case of ZrO₂ supported catalysts, the latter more largely deactivated than γ -Al₂O₃ supported ones due to strong sintering. The SSA of the washcoat decreased from 47 to 3 m²·g⁻¹ after exposure to 1100 °C for 8 h, thus providing an increase of T₅₀ (temperature of 50% methane conversion) by 175–190 °C [128].

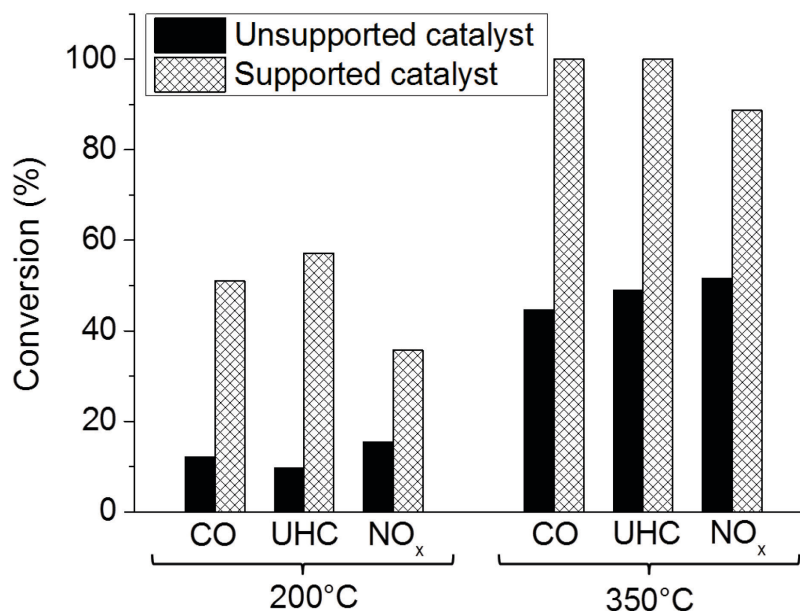
4. Implementation in TWC Converters

In the previous sections, we have demonstrated the promising TWC performance of powdered perovskite-type oxides and the possibility to prepare structured catalysts based on these materials. The activity of perovskite-type oxides logically increases with increasing amount of accessible active phase. Consequently, a higher efficiency is obtained on extruded and coated structured catalysts containing a higher loading of active component [104,120]. Accordingly, extruded catalysts with 70–80 wt% of active phase provide better conversion efficiencies in the kinetic regime than the coated unsupported catalysts that contain 5–30 wt% of active phase [101]. For real scale applications (e.g., automotive exhaust treatment), where high velocity streams have to be treated, washcoated catalysts are more advantageous than extruded ones due to minimized diffusion limitations and, hence, a larger fraction of accessible active phase.

Structured catalysts can be obtained by different synthesis methods. Non perovskite oxide layers prepared from precursors directly on the surfaces of a structured carrier are generally denser and have a lower SSA than those obtained by slurry-coating [84]. The difference is not so pronounced in the case of perovskite-type oxides due to the sudden release of large amounts of combustion related gases (NO_x, CO₂, H₂O) upon calcination. Thus, the precursor solution based synthesis produces a relatively porous catalytic perovskite-type oxide layer with a SSA, thickness and catalytic performance which are comparable to those of washcoated layers. However, the significant release of heat and combustion related corrosive gases during the calcination restricts large scale production. Perovskite-type materials synthesized directly on the substrate surface by soft chemistry have a relatively low stability at high temperatures which results in sintering and deactivation. For these reasons, washcoated structured catalysts prepared from high temperature stable powders (synthesized, for example by flame hydrolysis) are more appropriate for TWC applications [118]. Amongst all types of structured

catalysts, the best performance is obtained on washcoated supported ones containing a low amount (up to 6 wt% referred to the whole structured catalyst) of a highly dispersed perovskite-type oxide phase. Labhsetwar *et al.* [66] demonstrated the difference between supported and unsupported perovskite-type oxides coated on monoliths for TWC applications (Figure 13).

Figure 13. Comparison of CO, UHC, and NO_x conversions obtained on unsupported and supported La_{0.7}Sr_{0.3}Mn_{0.95}Pt_{0.05}O₃ washcoated cordierite honeycomb monoliths. Adapted from Labhsetwar *et al.* [66].



The authors also studied the suitability of these catalysts for real scale application by testing them on an engine dynamometer. With supported perovskite type oxides coated structured catalysts, high conversions of CO (82%), UHC (86%) and NO_x (71%) were obtained. Despite these promising results, the oxide support (typically γ -Al₂O₃) used to disperse the active phase has a lower thermal resistance than the perovskite-type oxide. The sintering of the oxide support results in the significant growth of supported perovskite-type oxide particles. Consequently, unsupported systems perform better than the supported ones after exposure to very high temperatures (*i.e.*, 1100 °C [101]).

The major advantage of perovskite-type oxides is that a large array of elements can be accommodated into the structure. This makes it possible to tailor catalytic properties of the materials for specific applications. However, this strength of perovskite-type oxides can be a drawback when it reacts with the substrate, binder or primer materials that are present in a TWC converter. This leads to decreased TWC activity. In extruded catalysts, such chemical interactions are not a serious issue owing to the high active phase content. Sadykov *et al.* have even reported advantages of such interactions: the conversion of the alumina binder into a hexa-aluminate phase upon solid state reaction with the perovskite-type oxide improves the mechanical strength of the extruded catalyst [90]. The strongest interactions are observed for supported structured catalysts due to the high dispersion of the active phase component [119]. In such catalysts, any alteration to the relatively low amount of active phase implies considerable activity loss. To prevent this, several authors have suggested that the surface of the oxide support should be thermally treated to achieve an inert upper layer prior to the deposition of

the active phase [131]. In agreement with this, α -Al₂O₃ was found to be less reactive than γ -Al₂O₃ to perovskite-type oxides [101]. Despite its reduced reactivity towards the active phase, α -Al₂O₃ has a significantly low SSA, which limits the dispersion of the supported perovskite-type oxide. Therefore, the deposition of a primer layer, e.g., La₂O₃, on a high SSA support appears to be the best option to protect the active perovskite-type oxide phase from chemical modifications while ensuring its sufficient dispersion.

Additional issues have to be taken into account for perovskite-type oxides to be implemented in TWC converters. For health and environmental reasons, certain elements cannot be included in the composition of a TWC due to their oxidation and volatilization under the high temperature exhaust environment comprising water vapor and corrosive gases. The volatile metal-based species are then potentially released in the environment through high space velocity exhaust gases. German clean air regulations identified that cobalt-based species formed under these conditions were potentially carcinogenic. On the same line, the “self-regenerative” perovskite-type oxide catalyst LaFe_{0.95}Pd_{0.05}O₃ was commercialized as a TWC component whereas LaFe_{0.57}Co_{0.38}Pd_{0.05}O₃ was not [14]. Though the thermal stability of perovskite-type oxides is high, their sulfur resistance is limited. The low sulfur tolerance of perovskite-type oxides can be overcome by appropriately designing the structured catalyst. A double layer configuration where the active perovskite-type oxide phase is located in the inner layer can avoid interactions between the active phase and sulfur-containing compounds and hence catalyst deactivation [14]. TWC converters containing a noble metal-based perovskite-type oxide with the double layer configuration shows better performance, over a wide range of space velocities, than a standard catalyst with a 1.5 times higher noble metal loading. As a result, self-regenerative Co-free perovskite-type catalysts were implemented in commercial TWC converters by Daihatsu Motor Co. Ltd. Around 3.2 million TWC converters based on this technology have been installed between 2002 and 2007 in Japan and in Europe [133].

Recently, solid foams have attracted particular attention as potential alternatives to honeycomb monoliths [134]. These sponge-like substrates contain interconnected and randomly-organized open pores in the millimeter-range. These foams can typically be made of the same constituting materials as monoliths and are characterized by their pore density, which can vary from 5 to 100 pores per inch (ppi). Compared to monoliths, the structure of foams creates higher pressure drops but allows radial mixing and enhanced turbulence [135]. Such features improve mass and heat transfers, which are crucial parameters in exhaust after-treatment applications. There are very few studies on perovskite-type oxides based foam catalysts [119,130] and none of them evaluates the performance of the foams in relation to the conventional honeycomb monoliths.

The multifunctional properties of perovskite-type oxides could also impart new possibilities to the TWC converters. For example, by exploiting the dielectric properties of perovskite-type oxides, TWC converters can be dielectrically-heated to minimize exhaust emissions during the cold start of a gasoline engine [87]. A cordierite monolith coated with LaCoO₃ exhibits rapid heat-up under microwave irradiation allowing to attain the 50% UHC conversion temperature within 15 s. Similarly, La_{0.8}Ce_{0.2}MnO₃ was reported as a dielectric material for the periodical regeneration of monolithic soot filters in diesel exhaust after-treatment systems [124]. Perovskite-type oxides are also studied for thermoelectric applications [22]: manganites, cuprates and cobaltites, which are known for their suitable catalytic performance, can be used to build thermoelectric oxide modules for the direct

conversion of heat into electricity [136]. As a consequence, an appropriately designed TWC converter made of a suitable perovskite-type oxide could simultaneously remove noxious compounds from the exhaust gases and recycle the waste heat into electric energy for the vehicle.

5. Conclusions

Perovskite-type oxides are reviewed in relation to their application in exhaust after-treatment technologies as three-way catalysts (TWC). The main advantage of these materials is their robust crystal structure that can be used to catalyze redox reactions due to their flexible oxygen content. The possibility to accommodate simultaneously different metal cations at A- and B-sites allows to tune the catalytic properties for a specific application such as TWC, which requires redox properties with high thermal stability. As such, perovskite-type oxides exhibit good oxidation activity which can be improved by including a fraction of noble metals like Pd, Pt, or Rh at the B-site. However, significant improvement in the oxidation activity of the materials is only observed when the noble metal is dislodged from the B-site of the crystal and forms metal nanoparticles of few nanometers at the surface. Recent studies demonstrate that the dislodged noble metal is not completely reintegrated into the perovskite crystal, questioning the self-regenerative property of the materials. The potential use of these materials for real scale TWC applications is studied by converting powder catalysts into structured ones such as monoliths or foams.

Acknowledgments

The authors are grateful to the COFUND program (EMPAPOSTDOCS project PCOFUND-GA-2010-267161) and the National Research Program SNF-NRP 62 “Smart Materials” (project no. 406240-126127) for their financial support. We also thank Gion Pirovino for his support.

Author Contributions

Sylvain Keav wrote the main text. Santhosh Kumar Matam contributed to Sections 4 and 5 and to improve the text. Davide Ferri wrote the abstract and corrected the work. Anke Weidenkaff is the responsible author and corrected the work.

Conflicts of Interest

The authors declare no conflict of interest.

References

1. Taylor, K.C. Automobile Catalytic Converters. *Stud. Surf. Sci. Catal.* **1987**, *30*, 97–116.
2. Trovarelli, A. *Catalysis by Ceria and Related Materials*, 1st ed.; Imperial College Press: London, UK, 2002.
3. Forster, P.; Ramaswamy, V.; Artaxo, P.; Berntsen, T.; Betts, R.; Fahey, D.W.; Haywood, J.; Lean, J.; Lowe, D.C.; Myhre, G.; *et al.* Changes in Atmospheric Constituents and in Radiative Forcing. In *Climate Change 2007: The Physical Science Basis. Contribution of Working Group I to the Fourth Assessment Report of the Intergovernmental Panel on Climate Change*; Solomon, S.,

- Qin, D., Manning, M., Chen, Z., Marquis, M., Averyt, K.B., Tynor, M., Miller, H.L., Eds.; Cambridge University Press: Cambridge, UK; New York, NY, USA, 2007; pp. 129–234.
- Fino, D.; Russo, N.; Saracco, G.; Specchia, V. Supported Pd-perovskite catalyst for CNG engines' exhaust gas treatment. *Prog. Solid State Chem.* **2007**, *35*, 501–511.
 - Yao, H.C.; Japar, S.; Shelef, M. Surface Interactions in the System Rh/Al₂O₃. *J. Catal.* **1977**, *50*, 407–418.
 - Libby, W.F. Promising Catalyst for Auto Exhaust. *Science* **1971**, *171*, 499–500.
 - Voorhoeve, R.J.H.; Remeika, J.P.; Freeland, P.E.; Matthias, B.T. Rare-Earth Oxides of Manganese and Cobalt Rival Platinum for the Treatment of Carbon Monoxide in Auto Exhaust. *Science* **1972**, *177*, 353–354.
 - Voorhoeve, R.J.H.; Remeika, J.P.; Johnson, D.W., Jr. Rare-Earth Manganites: Catalysts with Low Ammonia Yield in the Reduction of Nitrogen Oxides. *Science* **1973**, *180*, 62–64.
 - Voorhoeve, R.J.H.; Remeika, J.P.; Trimble, L.E. Perovskites containing ruthenium as catalysts for nitric oxide reduction. *Mater. Res. Bull.* **1974**, *9*, 1393–1404.
 - Voorhoeve, R.J.H.; Trimble, L.E. Exploration of perovskite-like catalysts: Ba₂CoWO₆ and Ba₂FeNbO₆ in NO reduction and CO oxidation. *Mater. Res. Bull.* **1974**, *9*, 655–666.
 - Gallagher, P.K.; Johnson, D.W., Jr.; Schrey, F. Studies of some supported perovskite oxidation catalysts. *Mater. Res. Bull.* **1974**, *9*, 1345–1352.
 - Tabata, K.; Misono, M. Elimination of pollutant gases—Oxidation of CO, reduction and decomposition of NO. *Catal. Today* **1990**, *8*, 249–261.
 - Guilhaume, N.; Primet, M. Three-Way Catalytic Activity and Oxygen Storage Capacity of Perovskite LaMn_{0.976}Rh_{0.024}O_{3+δ}. *J. Catal.* **1997**, *165*, 197–204.
 - Tanaka, H. An intelligent catalyst: The self-regenerative palladium-perovskite catalyst for automotive emissions control. *Catal. Surv. Asia* **2005**, *9*, 63–74.
 - Kim, C.H.; Qi, G.; Dahlberg, K.; Li, W. Strontium-Doped Perovskites Rival Platinum Catalysts for Treating NO_x in Simulated Diesel Exhaust. *Science* **2010**, *327*, 1624–1627.
 - Goldschmidt, V.M. Die Gesetze der Krystallochemie. *Die Naturwissenschaften* **1926**, *8*, 477–485.
 - Ebbinghaus, S.G.; Abicht, H.P.; Dronskowski, R.; Müller, T.; Reller, A.; Weidenkaff, A. Perovskite-related oxynitrides—Recent developments in synthesis, characterisation and investigations of physical properties. *Progr. Solid State Chem.* **2009**, *37*, 173–205.
 - Yoon, S.; Maegli, A.E.; Karvonen, L.; Matam, S.K.; Shkabko, A.; Riegg, S.; Großmann, T.; Ebbinghaus, S.G.; Pokrant, S.; Weidenkaff, A. Bandgap tuning in SrTi(N,O,F)₃ by anionic-lattice variation. *J. Solid State Chem.* **2013**, *206*, 226–232.
 - Weidenkaff, A.; Ebbinghaus, S.G.; Lippert, T.; Montenegro, M.J.; Soltmann, C.; Wessicken, R. Phase formation and phase transition of Ln_{1-x}Ca_xCoO_{3-δ} (Ln = La, Er) applied for bifunctional air electrodes. *Cryst. Eng.* **2002**, *5*, 449–457.
 - Weidenkaff, A. Preparation and Application of Nanostructured Perovskite Phases. *Adv. Eng. Mater.* **2004**, *6*, 709–714.
 - Raveau, B. The perovskite history: More than 60 years of research from the discovery of ferroelectricity to colossal magnetoresistance via high TC superconductivity. *Prog. Solid State Chem.* **2007**, *35*, 171–173.

22. Weidenkaff, A.; Robert, R.; Aguirre, M.; Bochet, L.; Lippert, T.; Canulescu, S. Development of thermoelectric oxides for renewable energy conversion technologies. *Renew. Energy* **2008**, *33*, 342–347.
23. Voorhoeve, R.J.H.; Johnson, D.W., Jr.; Remeika, J.P.; Gallagher, P.K. Perovskite Oxides: Materials Science in Catalysis. *Science* **1977**, *195*, 827–833.
24. Bhalla, A.S.; Guo, R.; Roy, R. The perovskite structure—A review of its role in ceramic science and technology. *Mater. Res. Innov.* **2000**, *4*, 3–26.
25. Peña, M.A.; Fierro, J.L.G. Chemical Structures and Performance of Perovskite Oxides. *Chem. Rev.* **2001**, *101*, 1981–2017.
26. Tejuca, L.G.; Fierro, J.L.G.; Tascón, J.M.D. Structure and Reactivity of Perovskite-Type Oxides. *Adv. Catal.* **1989**, *36*, 237–328.
27. Royer, S.; Duprez, D. Catalytic Oxidation of Carbon Monoxide over Transition Metal Oxides. *ChemCatChem* **2011**, *3*, 24–65.
28. Parravano, G. Ferroelectric Transitions and Heterogeneous Catalysis. *J. Chem. Phys.* **1952**, *20*, 342–343.
29. Dickens, P.G.; Whittingham, M.S. Recombination of oxygen atoms on oxide surfaces. Part 2.—Catalytic activities of the alkali metal tungsten bronzes. *Trans. Faraday Soc.* **1965**, *61*, 1226–1231.
30. Tascón, J.M.D.; Tejuca, L.G. Catalytic activity of perovskite-type oxides LaMeO_3 . *React. Kinet. Catal. Lett.* **1980**, *15*, 185–191.
31. Nitadori, T.; Ichiki, T.; Misono, M. Catalytic Properties of Perovskite-Type Mixed Oxides (ABO_3) Consisting of Rare Earth and 3d Transition Metals. The Roles of the A- and B-Site Ions. *Bull. Chem. Soc. Jpn.* **1988**, *61*, 621–626.
32. Panich, N.M.; Pirogova, G.N.; Korosteleva, R.I.; Voronin, Y.V. Oxidation of CO and hydrocarbons over perovskite-type complex oxides. *Russ. Chem. Bull.* **1999**, *48*, 694–697.
33. Voorhoeve, R.J.H.; Remeika, J.P.; Trimble, L.E.; Cooper, A.S.; Disalvo, F.J.; Gallagher, P.K. Perovskite-like $\text{La}_{1-x}\text{K}_x\text{MnO}_3$ and related compounds: Solid state chemistry and the catalysis of the reduction of NO by CO and H_2 . *J. Sol. State. Chem.* **1975**, *14*, 395–406.
34. Hackenberger, M.; Stephan, K.; Kießling, D.; Schmitz, W.; Wendt, G. Influence of the preparation conditions on the properties of perovskite-type oxide catalysts. *Solid State Ionics* **1997**, *101–103*, 1195–1200.
35. Giannakas, A.E.; Ladavos, A.K.; Pomonis, P.J. Preparation, characterization and investigation of catalytic activity for NO + CO reaction of LaMnO_3 and LaFeO_3 perovskites prepared via microemulsion method. *Appl. Catal. B* **2004**, *49*, 147–158.
36. Lu, Y.; Eyssler, A.; Otal, E.H.; Matam, S.K.; Brunko, O.; Weidenkaff, A.; Ferri, D. Influence of the synthesis method on the structure of Pd-substituted perovskite catalysts for methane oxidation. *Catal. Today* **2013**, *208*, 42–47.
37. Campagnoli, E.; Tavares, A.; Fabbrini, L.; Rossetti, I.; Dubitsky, Y.A.; Zaopo, A.; Forni, A. Effect of preparation method on activity and stability of LaMnO_3 and LaCoO_3 catalysts for the flameless combustion of methane. *Appl. Catal. B* **2005**, *55*, 133–139.

38. Oliva, C.; Bonoldi, L.; Cappelli, S.; Fabbrini, L.; Rossetti, I.; Forni, L. Effect of preparation parameters on SrTiO_{3±δ} catalyst for the flameless combustion of methane. *J. Mol. Catal. A* **2005**, *226*, 33–40.
39. Stephan, K.; Hackenberger, M.; Kiessling, D.; Wendt, G. Supported perovskite-type oxide catalysts for the total oxidation of chlorinated hydrocarbons. *Catal. Today* **1999**, *54*, 23–30.
40. Ran, R.; Wu, X.; Weng, D. Effect of complexing species in a sol-gel synthesis on the physicochemical properties of La_{0.7}Sr_{0.3}Mn_{0.7}Cu_{0.3}O_{3+λ} catalyst. *J. Alloys Compd.* **2006**, *414*, 169–174.
41. Kaliaguine, S.; van Neste, A. Process for Synthesizing Perovskites Using High Energy Milling. U.S. Patent 6,017,504, 25 January 2000.
42. Kaliaguine, S.; van Neste, A.; Szabo, V.; Gallot, J.E.; Bassir, M.; Muzychuk, R. Perovskite-type oxides synthesized by reactive grinding—Part I. Preparation and characterization. *Appl. Catal. A* **2001**, *209*, 345–358.
43. Royer, S.; Bérubé, F.; Kaliaguine, S. Effect of the synthesis conditions on the redox and catalytic properties in oxidation reactions of LaCo_{1-x}Fe_xO₃. *Appl. Catal. A* **2005**, *282*, 273–284.
44. Zhang, R.; Villanueva, A.; Alamdari, H.; Kaliaguine, S. Catalytic reduction of NO by propene over LaCo_{1-x}Cu_xO₃ perovskites synthesized by reactive grinding. *Appl. Catal. B* **2006**, *64*, 220–223.
45. Levasseur, B.; Kaliaguine, S. Methanol oxidation on LaBO₃ (B = Co, Mn, Fe) perovskite-type catalysts prepared by reactive grinding. *Appl. Catal. A* **2008**, *343*, 29–38.
46. Shu, J.; Kaliaguine, S. Well-dispersed perovskite-type oxidation catalysts. *Appl. Catal. B* **1998**, *16*, L303–L308.
47. Ran, R.; Wu, X.; Weng, D.; Fan, J. Oxygen storage capacity and structural properties of Ni-doped LaMnO₃ perovskites. *J. Alloys Compd.* **2013**, *577*, 288–294.
48. Chang, Y.F.; McCarty, J.G. Novel oxygen storage components for advanced catalysts for emission control in natural gas fueled vehicles. *Catal. Today* **1996**, *30*, 163–170.
49. Yamazoe, N.; Teraoka, Y.; Seiyama, T. TPD and XPS study on thermal behavior of adsorbed oxygen in La_{1-x}Sr_xCoO₃. *Chem. Lett.* **1981**, *10*, 1767–1770.
50. Kremenić, G.; Nieto, J.M.L.; Tascón, J.M.D.; Tejuca, L.G. Chemisorption and catalysis on LaMO₃ oxides. *J. Chem. Soc. Faraday Trans. 1* **1985**, *81*, 939–949.
51. Arai, H.; Yamada, T.; Eguchi, K.; Seiyama, T. Catalytic combustion of methane over various perovskite-type oxides. *Appl. Catal.* **1986**, *26*, 265–276.
52. Markova-Velichkova, M.; Lazarova, T.; Tumbalev, V.; Ivanov, G.; Kovacheva, D.; Stefanov, P.; Naydenov, A. Complete oxidation of hydrocarbons on YFeO₃ and LaFeO₃ catalysts. *Chem. Eng. J.* **2013**, *231*, 236–244.
53. Voorhoeve, R.J.H.; Remeika, J.P.; Trimble, L.E. Defect chemistry and catalysis in oxidation and reduction over perovskite-type oxides. *Ann. N. Y. Acad. Sci.* **1976**, *272*, 3–21.
54. Fierro, J.L.G. Structure and composition of perovskite surface in relation to adsorption and catalytic properties. *Catal. Today* **1990**, *8*, 153–174.
55. Tascón, J.M.D.; Fierro, J.L.G.; Tejuca, L.G. Kinetics and Mechanism of CO Oxidation on LaCoO₃. *Z. Phys. Chem.* **1981**, *124*, 249–257.

56. Tascón, J.M.D.; Tejuca, L.G. Adsorption of CO₂ on the perovskite-type oxide LaCoO₃. *J. Chem. Soc. Faraday Trans. 1* **1981**, *77*, 591–602.
57. Forni, L.; Oliva, C.; Barzetti, T.; Selli, E.; Ezerets, A.M.; Vishniakov, A.V. FT-IR and EPR spectroscopic analysis of La_{1-x}Ce_xCoO₃ perovskite-like catalysts for NO reduction by CO. *Appl. Catal. B* **1997**, *13*, 35–43.
58. Harada, T.; Teraoka, Y.; Kagawa, S. Perovskite-type oxides as catalysts for selective reduction of nitric oxide by ethylene. *Appl. Surf. Sci.* **1997**, *121–122*, 505–508.
59. Yu Yao, Y.-F. The oxidation of hydrocarbons and CO over metal oxides: IV. Perovskite-type oxides. *J. Catal.* **1975**, *36*, 266–275.
60. Jovanovic, D.; Dondur, V.; Terlecki-Baricevic, A.; Grbic, B. Three-way activity and sulfur tolerance of single phase perovskites. *Stud. Surf. Sci. Catal.* **1991**, *71*, 371–379.
61. Gallagher, P.K.; Johnson, D.W., Jr.; Vogel, E.M.; Schrey, F. Effect of the Pt content of La_{0.7}Pb_{0.3}MnO₃ on its catalytic activity for the oxidation of CO in the presence of SO₂. *Mat. Res. Bull.* **1975**, *10*, 623–628.
62. Tzimpilis, E.; Moschoudis, N.; Stoukides, M.; Bekiaroglou, P. Ageing and SO₂ resistance of Pd containing perovskite-type oxides. *Appl. Catal. B* **2009**, *87*, 9–17.
63. Tzimpilis, E.; Moschoudis, N.; Stoukides, M.; Bekiaroglou, P. Preparation, active phase composition and Pd content of perovskite-type oxides. *Appl. Catal. B* **2008**, *84*, 607–615.
64. Mondragón Rodríguez, G.C.; Kelm, K.; Heikens, S.; Grünert, W.; Saruhan, B. Pd-integrated perovskites for TWC applications: Synthesis, microstructure and N₂O-selectivity. *Catal. Today* **2012**, *184*, 184–191.
65. Sorenson, S.C.; Wronkiewicz, J.A.; Sis, L.B.; Wirtz, G.P. Properties of LaCoO₃ as a Catalyst in Engine Exhaust Gases. *Am. Ceram. Soc. Bull.* **1974**, *53*, 446–449.
66. Labhsetwar, N.K.; Watanabe, A.; Biniwale, R.B.; Kumar, R.; Mitsuhashi, T. Alumina supported, perovskite oxide based catalytic materials and their auto-exhaust application. *Appl. Catal. B* **2001**, *33*, 165–173.
67. Tanaka, H.; Mizuno, N.; Misono, M. Catalytic activity and structural stability of La_{0.9}Ce_{0.1}Co_{1-x}Fe_xO₃ perovskite catalysts for automotive emission control. *Appl. Catal. A* **2003**, *244*, 371–382.
68. Bradow, R.; Jovanović, D.; Petrović, S.; Jovanović, Ž.; Terlecki-Baričević, A. Ruthenium Perovskite Catalysts for Lean NO_x Automotive Emission Control. *Ind. Eng. Chem. Res.* **1995**, *34*, 1929–1932.
69. Shelef, M.; Gandhi, H.S. The Reduction of Nitric Oxide in Automobile Emissions—Stabilisation of catalysts containing ruthenium. *Platin. Met. Rev.* **1974**, *18*, 2–14.
70. Nishihata, Y.; Mizuki, J.; Akao, T.; Tanaka, H.; Uenishi, M.; Kimura, M.; Okamoto, T.; Hamada, N. Self-regeneration of a Pd-perovskite catalyst for automotive emissions control. *Nature* **2002**, *418*, 164–167.
71. Tanaka, H.; Tan, I.; Uenishi, M.; Kimura, M.; Dohmae, K. Regeneration of palladium subsequent to solid solution and segregation in a perovskite catalyst: An intelligent catalyst. *Top. Catal.* **2001**, *16/17*, 63–70.
72. Uenishi, M.; Taniguchi, M.; Tanaka, H.; Kimura, M.; Nishihata, Y.; Mizuki, J.; Kobayashi, T. Redox behavior of palladium at start-up in the Perovskite-type LaFePdO_x automotive catalysts showing a self-regenerative function. *Appl. Catal. B* **2005**, *57*, 267–273.

73. Uenishi, M.; Tanaka, H.; Taniguchi, M.; Tan, I.; Sakamoto, Y.; Matsunaga, S.; Yokota, K.; Kobayashi, T. The reducing capability of palladium segregated from perovskite-type LaFePdO_x automotive catalysts. *Appl. Catal. A* **2005**, *296*, 114–119.
74. Tanaka, H.; Taniguchi, M.; Kajita, N.; Uenishi, M.; Tan, I.; Sato, N.; Narita, K.; Kimura, M. Design of the intelligent catalyst for Japan ULEV standard. *Top. Catal.* **2004**, *30/31*, 389–396.
75. Tanaka, H.; Taniguchi, M.; Uenishi, M.; Kajita, N.; Tan, I.; Nishihata, Y.; Mizuki, J.; Narita, K.; Kimura, M.; Kaneko, K. Self-Regenerating Rh- and Pt-Based Perovskite Catalysts for Automotive-Emissions Control. *Angew. Chem. Int. Ed.* **2006**, *45*, 5998–6002.
76. Dacquin, J.P.; Cabié, M.; Henry, C.R.; Lancelot, C.; Dujardin, C.; Raouf, S.R.; Granger, P. Structural changes of nano-Pt particles during thermal ageing: Support-induced effect and related impact on the catalytic performances. *J. Catal.* **2010**, *270*, 299–309.
77. Dacquin, J.P.; Lancelot, C.; Dujardin, C.; Cordier-Robert, C.; Granger, P. Support-Induced Effects of LaFeO₃ Perovskite on the Catalytic Performances of Supported Pt Catalysts in DeNO_x Applications. *J. Phys. Chem. C* **2011**, *115*, 1911–1921.
78. Katz, M.B.; Graham, G.W.; Duan, Y.; Liu, H.; Adamo, C.; Schlom, D.G.; Pan, X. Self-Regeneration of Pd-LaFeO₃ Catalysts: New Insight from Atomic-Resolution Electron Microscopy. *J. Am. Chem. Soc.* **2011**, *133*, 18090–18093.
79. Katz, M.B.; Zhang, S.; Duan, Y.; Wang, H.; Fang, M.; Zhang, K.; Li, B.; Graham, G.W.; Pan, X. Reversible precipitation/dissolution of precious-metal clusters in perovskite-based catalyst materials: Bulk *versus* surface re-dispersion. *J. Catal.* **2012**, *293*, 145–148.
80. Zhou, K.; Chen, H.; Tian, Q.; Hao, Z.; Shen, D.; Xu, X. Pd-containing perovskite-type oxides used for three-way catalysts. *J. Mol. Catal. A* **2002**, *189*, 225–232.
81. Lu, Y.; Michalow, K.A.; Matam, S.K.; Winkler, A.; Maegli, A.E.; Yoon, S.; Heel, A.; Weidenkaff, A.; Ferri, D. Methane abatement under stoichiometric conditions on perovskite-supported palladium catalysts prepared by flame spray synthesis. *Appl. Catal. B* **2014**, *144*, 631–643.
82. Nijhuis, T.A.; Beers, A.E.W.; Vergunst, T.; Hoek, I.; Kapteijn, F.; Moulijn, J.A. Preparation of monolithic catalysts. *Catal. Rev. Sci. Eng.* **2001**, *43*, 345–380.
83. Tomašić, V.; Jović, F. State-of-the-art in the monolithic catalysts/reactors. *Appl. Catal. A* **2006**, *311*, 112–121.
84. Meille, V. Review on methods to deposit catalysts on structured surfaces. *Appl. Catal. A* **2006**, *315*, 1–17.
85. Avila, P.; Montes, M.; Miró, E.E. Monolithic reactors for environmental applications: A review on preparation technologies. *Chem. Eng. J.* **2005**, *109*, 11–36.
86. Lachman, I.M.; Williams, J.L. Extruded Monolithic Catalysts Supports. *Catal. Today* **1992**, *14*, 317–329.
87. Bardhan, P. Ceramic honeycomb filters and catalysts. *Curr. Opin. Solid State Mater. Sci.* **1997**, *2*, 577–583.
88. Isupova, L.A.; Sadykov, V.A.; Tikhov, S.F.; Kimkhai, O.N.; Kovalenko, O.N.; Kustova, G.N.; Ovsyannikova, I.A.; Dovbii, Z.A.; Kryukova, G.N.; Rozovskii, A.Y.; *et al.* Monolith perovskite catalysts for environmentally benign fuels combustion and toxic wastes incineration. *Catal. Today* **1996**, *27*, 249–256.

89. Isupova, L.A.; Sadykov, V.A.; Solovyova, L.P.; Andrianova, M.P.; Ivanov, V.P.; Kryukova, G.N.; Kolomiichuk, V.N.; Avvakumov, E.G.; Pauli, I.A.; Andryushkova, O.V.; *et al.* Monolith perovskite catalysts of honeycomb structure for fuel combustion. *Stud. Surf. Sci. Catal.* **1995**, *91*, 637–645.
90. Sadykov, V.A.; Isupova, L.A.; Tikhov, S.F.; Kimkhai, O.N. Perovskite catalysts: High surface area powders synthesis, monolith shaping and high-temperature applications. *Mat. Res. Soc. Symp. Proc.* **1995**, *368*, 293–298.
91. Isupova, L.A.; Alikina, G.M.; Snegurenko, O.I.; Sadykov, V.A.; Tsybulya, S.V. Monolith honeycomb mixed oxide catalysts for methane oxidation. *Appl. Catal. B* **1999**, *21*, 171–181.
92. Isupova, L.A.; Sadykov, V.A.; Alikina, G.M.; Snegurenko, O.I.; Tsybulya, S.V.; Salanov, A.N.; Rogov, V.A. Monolith honeycomb mixed oxide catalysts for methane oxidation. *Stud. Surf. Sci. Catal.* **2000**, *130*, 3783–3788.
93. Ciambelli, P.; Palma, V.; Tikhov, S.F.; Sadykov, V.A.; Isupova, L.A.; Lisi, L. Catalytic activity of powder and monolith perovskites in methane combustion. *Catal. Today* **1999**, *47*, 199–207.
94. Schneider, R.; Kiessling, D.; Wendt, G.; Burckhardt, W.; Winterstein, G. Perovskite-type oxide monolithic catalysts for combustion of chlorinated hydrocarbons. *Catal. Today* **1999**, *47*, 429–435.
95. Khan, H.R.; Frey, H. R.f. plasma spray deposition of LaMO_x ($M = \text{Co}, \text{Mn}, \text{Ni}$) films and the investigations of structure, morphology and the catalytic oxidation of CO and C_3H_8 . *J. Alloys Compd.* **1993**, *190*, 209–217.
96. Bahlawane, N.; Ngamou, P.H.T.; Kohse-Höinghaus, K. Structure, Electrical Properties, and Surface Reactivity of CVD-Made Functional Complex Oxides. *J. Electrochem. Soc.* **2010**, *157*, D16–D20.
97. Sansernnivet, M.; Laosiripojana, N.; Assabumrungrat, S.; Charojrochkul, S. Fabrication of $\text{La}_{0.8}\text{Sr}_{0.2}\text{CrO}_3$ -based Perovskite Film via Flame-Assisted Vapor Deposition for H_2 Production by Reforming. *Chem. Vap. Depos.* **2010**, *16*, 311–321.
98. Jarligo, M.O.; Mauer, G.; Bram, M.; Baumann, S.; Vaßen, R. Plasma Spray Physical Vapor Deposition of $\text{La}_{1-x}\text{Sr}_x\text{Co}_y\text{Fe}_{1-y}\text{O}_{3-\delta}$ Thin-Film Oxygen Transport Membrane on Porous Metallic Supports. *J. Therm. Spray Technol.* **2014**, *23*, 213–219.
99. Uusi-Esko, K.; Karppinen, M. Extensive Series of Hexagonal and Orthorhombic RMnO_3 ($R = \text{Y}, \text{La}, \text{Sm}, \text{Tb}, \text{Yb}, \text{Lu}$) Thin Films by Atomic Layer Deposition. *Chem. Mater.* **2011**, *23*, 1835–1840.
100. Schneider, R.; Kiessling, D.; Wendt, G. Cordierite monolith supported perovskite-type oxides catalysts for the total oxidation of chlorinated hydrocarbons. *Appl. Catal. B* **2000**, *28*, 187–195.
101. Isupova, L.A.; Alikina, G.M.; Tsybulya, S.V.; Salanov, A.N.; Blodyreva, N.N.; Rusina, E.S.; Ovsyannikova, I.A.; Rogov, V.A.; Bunina, R.V.; Sadykov, V.A. Honeycomb-supported perovskite catalysts for high-temperature processes. *Catal. Today* **2002**, *75*, 305–315.
102. Li, L.; Shen, X.; Wang, P.; Meng, X.; Song, F. Soot capture and combustion for perovskite La-Mn-O based catalysts coated on honeycomb ceramic in practical diesel exhaust. *Appl. Surf. Sci.* **2011**, *257*, 9519–9524.
103. Isupova, L.A.; Sutormina, E.F.; Kulilovskaya, N.A.; Plyasova, L.M.; Rudina, N.A.; Ovsyannikova, I.A.; Zootarskii, I.A.; Sadykov, V.A. Honeycomb supported perovskite catalysts for ammonia oxidation processes. *Catal. Today* **2005**, *105*, 429–435.

104. Sannino, D.; Vaiano, V.; Ciambelli, P.; Isupova, L.A. Structured catalysts for photo-Fenton oxidation of acetic acid. *Catal. Today* **2011**, *161*, 255–259.
105. Pechini, M.P. Method of preparing lead and alkaline earth titanates and niobates and coating method using the same to form a capacitor. U.S. Patent 3,330,697, 11 July 1967.
106. Qi, A.; Wang, S.; Fu, G.; Ni, C.; Wu, D. La-Ce-Ni-O monolithic perovskite catalysts potential for gasoline autothermal reforming system. *Appl. Catal. A* **2005**, *281*, 233–246.
107. Vergunst, T.; Kapteijn, F.; Moulijn, J.A. Monolithic catalysts—Non-uniform active phase distribution by impregnation. *Appl. Catal. A* **2001**, *213*, 179–187.
108. Cauda, E.; Fino, D.; Saracco, G.; Specchia, V. Nanosized Pt-perovskite catalyst for the regeneration of a wall-flow filter for soot removal from diesel exhaust gases. *Top. Catal.* **2004**, *30/31*, 299–303.
109. Russo, N.; Furfori, S.; Fino, D.; Saracco, G.; Specchia, V. Lanthanum cobaltite catalysts for diesel soot combustion. *Appl. Catal. B* **2008**, *83*, 85–95.
110. Russo, N.; Fino, D.; Saracco, G.; Specchia, V. Promotion effect of Au on perovskite catalysts for the regeneration of diesel particulate filters. *Catal. Today* **2008**, *137*, 306–311.
111. Mescia, D.; Caroca, J.C.; Russo, N.; Labhsetwar, N.; Fino, D.; Saracco, G.; Specchia, V. Towards a single brick solution for the abatement of NO_x and soot from diesel engine exhausts. *Catal. Today* **2008**, *137*, 300–305.
112. Fino, D.; Russo, N.; Cauda, E.; Saracco, G.; Specchia, V. La-Li-Cr perovskite catalysts for diesel particulate combustion. *Catal. Today* **2006**, *114*, 31–39.
113. Furfori, S.; Russo, N.; Fino, D.; Saracco, G.; Specchia, V. NO SCR reduction by hydrogen generated in line on perovskite-type catalysts for automotive diesel exhaust gas treatment. *Chem. Eng. Sci.* **2010**, *65*, 120–127.
114. Cauda, E.; Fino, D.; Saracco, G.; Specchia, V. Preparation and regeneration of a catalytic diesel particulate filter. *Chem. Eng. Sci.* **2007**, *62*, 5182–5185.
115. Mescia, D.; Cauda, E.; Russo, N.; Fino, D.; Saracco, G.; Specchia, V. Towards practical application of lanthanum chromite catalysts for diesel particulate combustion. *Catal. Today* **2006**, *117*, 369–375.
116. Fino, D.; Fino, P.; Saracco, G.; Specchia, V. Innovative means for the catalytic regeneration of particulate traps for diesel exhaust cleaning. *Chem. Eng. Sci.* **2003**, *58*, 951–958.
117. Arendt, E.; Maione, A.; Klisinska, A.; Sanz, O.; Montes, M.; Suarez, S.; Blanco, J.; Ruiz, P. Structuration of LaMnO₃ perovskite catalysts on ceramic and metallic monoliths: Physico-chemical characterisation and catalytic activity in methane combustion. *Appl. Catal. A* **2008**, *339*, 1–14.
118. Fabbrini, L.; Rossetti, I.; Forni, L. Effect of primer on honeycomb-supported La_{0.9}Ce_{0.1}CoO_{3±δ} perovskite for methane catalytic flameless combustion. *Appl. Catal. B* **2003**, *44*, 107–116.
119. Podyacheva, O.Y.; Ketov, A.A.; Ismagilov, Z.R.; Ushakov, V.A.; Bos, A.; Veringa, H.J. Metal foam supported perovskite catalysts. *React. Kinet. Catal. Lett.* **1997**, *60*, 243–250.
120. Forni, L.; Rossetti, I. Catalytic combustion of hydrocarbons over perovskites. *Appl. Catal. B* **2002**, *38*, 29–37.
121. Fabbrini, L.; Rossetti, I.; Forni, L. La₂O₃ as primer for supporting La_{0.9}Ce_{0.1}CoO_{3±δ} on cordieritic honeycombs. *Appl. Catal. B* **2005**, *56*, 221–227.

122. Fabbrini, L.; Rossetti, I.; Forni, L. Effect of honeycomb supporting on activity of $\text{LaBO}_{3+\delta}$ perovskite-like catalysts for methane flameless combustion. *Appl. Catal. B* **2006**, *63*, 131–136.
123. Arai, H.; Machida, M. Thermal stabilization of catalyst supports and their application to high-temperature catalytic combustion. *Appl. Catal. A* **1996**, *138*, 161–176.
124. Zhang-Steenwinkel, Y.; van der Zande, L.M.; Castricum, H.L.; Bliiek, A.; van den Brink, R.W.; Elzinga, G.D. Microwave-assisted *in-situ* regeneration of a perovskite coated diesel soot filter. *Chem. Eng. Sci.* **2005**, *60*, 797–804.
125. Kucharczyk, B.; Tylus, W. Effect of Pd or Ag additive on the activity and stability of monolithic LaCoO_3 perovskites for catalytic combustion of methane. *Catal. Today* **2004**, *90*, 121–126.
126. Kucharczyk, B.; Tylus, W. Partial substitution of lanthanum with silver in the LaMnO_3 perovskite: Effect of the modification on the activity of monolithic catalysts in the reactions of methane and carbon oxide oxidation. *Appl. Catal. A* **2008**, *335*, 28–36.
127. Cimino, S.; Pirone, R.; Russo, G. Thermal Stability of Perovskite-Based Monolithic Reactors in the Catalytic Combustion of Methane. *Ind. Eng. Chem. Res.* **2001**, *40*, 80–85.
128. Cimino, S.; Pirone, R.; Lisi, L. Zirconia supported LaMnO_3 monoliths for the catalytic combustion of methane. *Appl. Catal. B* **2002**, *35*, 243–254.
129. Cimino, S.; Lisi, L.; Pirone, R.; Russo, G.; Turco, M. Methane combustion on perovskites-based structured catalysts. *Catal. Today* **2000**, *59*, 19–31.
130. Jiratova, K.; Moravkova, L.; Malecha, J.; Koutsky, B. Ceramic foam-supported perovskites as catalysts for combustion of methane. *Collect. Czechoslov. Chem. Commun.* **1997**, *62*, 875–883.
131. Zwinkels, M.F.M.; Haussner, O.; Govind Menon, P.; Järås, S.G. Preparation and characterization of LaCrO_3 and Cr_2O_3 methane combustion catalysts supported on $\text{LaAl}_{11}\text{O}_{18}$ - and Al_2O_3 -coated monoliths. *Catal. Today* **1999**, *47*, 73–82.
132. Cimino, S.; Di Benedetto, A.; Pirone, R.; Russo, G. Transient behaviour of perovskite-based monolithic reactors in the catalytic combustion of methane. *Catal. Today* **2001**, *69*, 95–103.
133. Muroi, T.; Nojiri, N.; Deguchi, T. Recent progress in catalytic technology in Japan—II (1994–2009). *Appl. Catal. A* **2010**, *389*, 27–45.
134. Dimopoulos Eggenschwiler, P.; Tsinoglou, D.N.; Seyfert, J.; Bach, C.; Vogt, U.; Gorbar, M. Ceramic foam substrates for automotive catalyst applications: Fluid mechanic analysis. *Exp. Fluids* **2009**, *47*, 209–222.
135. Patcas, F.C.; Garrido, G.I.; Kraushaar-Czanetzki, B. CO oxidation over structured carriers: A comparison of ceramic foams, honeycombs and beads. *Chem. Eng. Sci.* **2007**, *62*, 3984–3990.
136. Populoh, S.; Trottmann, M.; Brunko, O.C.; Thiel, P.; Weidenkaff, A. Construction of a high temperature TEG measurement system for the evaluation of thermoelectric oxide modules. *Funct. Mater. Lett.* **2013**, *6*, doi:10.1142/S1793604713400122.